JPET Fast Forward. Published on August 22, 2016 as DOI: 10.1124/jpet.116.235127
This article has not been copyedited and formatted. The final version may differ from this version.

[JPET # 235127]

Myeloperoxidase inhibition increases neurogenesis after ischemic stroke

HyeonJu Kim, Ying Wei, Ji Yong Lee, Yue Wu, Yi Zheng, Michael A. Moskowitz, and John W. Chen

Center for System Biology and Institute for Innovation in Imaging, Massachusetts General Hospital, Harvard Medical School, Boston, MA (H.-J.K., J.-Y.L., J.W.C), and Neuroscience Center, Massachusetts General Hospital, Harvard Medical School, Boston, MA (W.Y., Y.W., Y.Z., M.A.M).

JPET Fast Forward. Published on August 22, 2016 as DOI: 10.1124/jpet.116.235127
This article has not been copyedited and formatted. The final version may differ from this version.

[JPET # 235127]

Running title: MPO inhibition increases neurogenesis after stroke

Corresponding author:

John W. Chen, MD, PhD
Massachusetts General Hospital, Harvard Medical School
Richard B. Simches Research Center
185 Cambridge Street
Boston, MA, 02114, USA
Tel: 617-643-7071
Fax: 617- 643-6133
E-mail: Jwchen@mgh.harvard.edu

Number of text pages: 33
Number of tables: 0
Number of figures: 12
Number of references: 65
Number of words in the abstract: 234
Number of words in the introduction: 509
Number of words in discussion: 1070

Abbreviations:

ABAH, 4-aminobenzoic acid hydrazide; AcH3, acetylated H3; AcH4, acetylated H4; ANOVA, analysis of variance; aSVZ, anterior subventricular zone; BBB, blood-brain barrier; BDNF, brain-derived neurotrophic factor; BrdU, 5-bromo-2' deoxyuridine; CCA, common carotid artery; CNS, central nervous system; CXCR4, CXC chemokine receptor-4; DCX, doublecortin; DG, dentate gyrus; DNA, deoxyribonucleic acid, ECA, external carotid artery; FITC, fluorescein isothiocyanate; GFAP, glial fibrillary acidic protein; HDAC, Histone deacetylase; HOCl, hypochlorous acid; HPF, high power field; Iba-1, a calcium-binding adaptor molecular 1, ICA, internal carotid artery; LDF, Laser Doppler Flowmetry; LPS, lipopolysaccharide; MMPs, Matrix metalloproteinases; MMP-9, Matrix metallopeptidase-9; MPO, myeloperoxidase; $MPO^{-/-}$, MPO knock out; NeuN, neuronal nuclei; NOX, NADPH oxidase; NSC, neural stem cells; OB, olfactory bulb; PBS, phosphate-buffered saline; Pcox, parietal cortex; p-CREB, phospho-cAMP response element-binding protein; rCBF, regional cerebral blood flow; ROS, reactive oxygen species; SDF-1, stromal cell-derived factor 1; SGL, subgranular layer; SVZ, subventricular zone; tMCAO, transient middle cerebral artery occlusion; TNF, tumor necrosis factor.

JPET Fast Forward. Published on August 22, 2016 as DOI: 10.1124/jpet.116.235127
This article has not been copyedited and formatted. The final version may differ from this version.

[JPET # 235127]

Section options: Drug Discovery and Translational Medicine

ABSTRACT

The relationship between inflammation and neurogenesis in stroke is currently not well understood. Focal ischemia enhances cell proliferation and neurogenesis in the neurogenic regions including the subventricular zone (SVZ), dentate gyrus (DG) as well as non-neurogenic striatum, cortex in the ischemic hemisphere. Myeloperoxidase (MPO) is a potent oxidizing enzyme secreted during inflammation by activated leukocytes and its enzymatic activity is highly elevated after stroke. In this study, we investigated whether inhibition of MPO activity by a specific irreversible inhibitor, 4-aminobenzoic acid hydrazide (ABAH) or $MPO^{-/-}$ mice can increase neurogenesis after transient middle cerebral artery occlusion (tMCAO) in mice. ABAH administration increased the number of proliferating 5-bromo-2' deoxyuridine (BrdU)-positive cells expressing markers for neural stems cells, astrocytes, neuroprogenitors (Nestin), and neuroblasts (doublecortin) in the ischemic SVZ, anterior SVZ (aSVZ), striatum and cortex. MPO inhibition also increased levels of brain-derived neurotrophic factor (BDNF), phospho-cAMP response element-binding protein (pCREB Ser133), acetylated H3 (AcH3), and NeuN to promote neurogenesis in the ischemic SVZ. ABAH treatment also increased chemokine CXC receptor 4 (CXCR 4) expression in the ischemic SVZ. MPO-deficient mice treated with vehicle or ABAH both showed similar effects on the number of $BrdU^{+}$ cells in the ischemic hemisphere, demonstrating that ABAH is specific to MPO. Taken together, our results underscore a detrimental role of MPO activity to post-ischemia neurogenesis and that a strategy to inhibit MPO activity can increase cell proliferation and improve neurogenesis after ischemic stroke.

INTRODUCTION

Adult neurogenesis produces newborn neurons from neural stem cells (NSC)/neural progenitors in the adult neurogenic niche of the central nervous system (CNS) (Ming and Song, 2011; Zhao et al., 2008). Two neurogenic areas in the brain are the subventricular zone (SVZ) and the hippocampal dentate gyrus (DG) (Alvarez-Buylla and Garcia-Verdugo, 2002). Focal cerebral ischemia increases neurogenesis in the SVZ and DG (Arvidsson et al., 2002; Ohab et al., 2006; Thored et al., 2006; Yamashita et al., 2006; Zhang et al., 2007). While most of the neural stem cells die shortly after proliferation, in human stroke patients, surviving neural stem cells in the SVZ can differentiate into neuroblasts and migrate into the olfactory bulb (OB) (Curtis et al, 2007). The neuroblasts can further migrate to ischemic striatum and cortex and mature into functional neurons (Jin et al., 2003; Zhang et al., 2004; Kim et al., 2009; Tobin et al., 2014). Ischemic brain injury also results in a rapid increase of inflammatory cells such as neutrophils, monocytes and activated microglia in the damaged brain. These pro-inflammatory cells release and generate reactive oxygen species (ROS), cytokines and chemokines leading to detrimental effects after stroke (Chamorro and Hallenbeck, 2006; Wang et al., 2007; Lo et al., 2010). Myeloperoxidase (MPO) is a hemoprotein that is abundantly expressed by active neutrophils, monocytes, macrophages and microglia (Lau & Baldus, 2006). MPO has been implicated in stroke, Alzheimer's disease and multiple sclerosis (Breckwoldt et al., 2008; Chen et al., 2008; Maki et al., 2009). MPO can generate free radicals by catalyzing the conversion of H_2O_2 and chloride into the potent hypochlorous acid (HOCl) which can generate tyrosyl radicals and oxidize lipid (Heinecke et al., 2002; Zhang et al., 2002). These MPO-derived oxidants trigger cellular dysfunction through its catalytic activity, which contributes to tissue injury (Nussbaum et al., 2013). MPO also has been found to delay neutrophil apoptosis and resolution of

inflammation (El Kebir and Filep; 2013). MPO itself can also function to recruit neutrophils (Klinke et al., 2011), propagating the inflammatory cascade. Elevated MPO expression has been found to persist for 21 days after stroke in a mouse model (Breckwoldt et al., 2008), and inhibiting MPO activity markedly decreased infarct size, even when given during the subacute stage of stroke (Forghani et al., 2014).

While neurogenesis is increased after stroke, the relationship between inflammation and neurogenesis in stroke is currently not well understood (Tobin et al, 2014). However, it is known that the inflammatory endotoxin lipopolysaccharide (LPS) can increase microglial activation (Monje et al., 2003) and inhibit neurogenesis (Ekdahl et al., 2003; Cacci et al., 2008). Microglial activation and neutrophil infiltration can also produce pro-inflammatory cytokine such as IL-1β, tumor necrosis factor (TNF), and IL-6, which decrease newborn cell survival (Kohman and Rhodes, 2013). Further, TNF is upregulated in stroke and deletion of the TNF-R1 receptor enhances progenitor proliferation (Iosif et al., 2008). Therefore, we hypothesize that MPO, because of its key roles in inflammatory damage, impacts neurogenesis, and consequently its inhibition by the specific irreversible inhibitor 4-aminobenzoic acid hydrazide (ABAH) can increase neurogenesis after ischemic stroke.

MATERIALS AND METHODS

Animal Care

The Massachusetts General Hospital Animal Care and Use Committee approved all animal experiments following National Institute of Health guidelines on the care and use of animals. C57BL/6J male mice (8-10 weeks, 23-25g) (n=167) and $MPO^{-/-}$ male mice (8-10 weeks, n=23, 13^{th} generation backcross on the C57BL/6J background) were purchased from Jackson

JPET Fast Forward. Published on August 22, 2016 as DOI: 10.1124/jpet.116.235127
This article has not been copyedited and formatted. The final version may differ from this version.

Laboratory (Bar Harbor, MA, USA). Mice were divided randomly into three groups: (i) sham-operated control animals (n=53), (ii) ischemia induced by transient middle cerebral artery occlusion (tMCAO) followed by saline-treatment (n=57), and (iii) tMCAO-induced ischemia followed by ABAH-treatment (n=57). Male mice 8-10 weeks of age were used in the experiments. Food and water were freely accessible to the mice and the holding rooms were maintained on a 12 h light/dark cycle. Mice were tested for neurobehavioral deficits and then sacrificed on day 7 or 21 after tMCAO for immunohistochemistry.

Focal Cerebral ischemia model

Focal cerebral ischemia was induced by transiently occluding the right middle cerebral artery for 30 min followed by reperfusion in mice as described previously (Breckwoldt et al, 2008). The mice were anesthetized by 1.5-2.0% isoflurane (Baxter health care corporation, Deerfield, IL, USA) with mixture of 30% O_2 and 70% N_2O as described previously. Under a dissecting microscope, a ventral midline neck incision was performed and the right carotid bifurcation was exposed. We carefully isolated the common carotid artery (CCA), external carotid artery (ECA) and internal carotid artery (ICA) from surrounding connective tissues. A small nick was made in the ECA stump and a 7-0 fine surgical nylon monofilament (diameter 0.19-0.20 mm) coated with silicon (Cat # 7019PK5Re, Doccol Co., Sharon, MA, USA) was inserted into the right ICA lumen through the ECA stump and advanced up to the MCA origin at the Circle of Willis. To monitor local blood flow in the MCA territory, we placed the microtip perpendicularly glued on the surface of the ischemic right parietal skull. The coordinates of the Laser-Doppler placement was 5 mm lateral and 1mm posterior to the bregma. We confirmed severe regional cerebral blood flow (rCBF) reduction by using Laser Doppler Flowmetry (LDF) (AD instruments, model: ML191, Colorado Springs, CO, USA). The LDF reduction was

JPET Fast Forward. Published on August 22, 2016 as DOI: 10.1124/jpet.116.235127
This article has not been copyedited and formatted. The final version may differ from this version.

normalized to the starting baseline. After 30 min occlusion, the suture was gently withdrawn for reperfusion and then ECA was ligated. Reperfusion was confirmed by increase of rCBF (approximately 70% ratio), which reached pre-ischemic level within 5 min. During the surgery, mice were maintained at 37°C by using heating pad (FHC Bowdoinham, ME, USA). After that, mice were kept in an incubator and allowed to recovery for 2 h at 35°C. Sham-operated animals were treated identically except suture was not inserted in the mice.

ABAH treatment and BrdU administration

The specific irreversible MPO inhibitor, 4-amino benzoic acid hydrazide (ABAH, 40 mg/kg, Sigma-Aldrich, St Louis, MO) was intraperitoneally administrated to the treated groups at 8 h after stroke and then twice daily up to day 7 or 21 following stroke (ABAH structure, Supplementary Fig. 1A). Another group of mice was treated with normal saline as control on the same schedule. The optimal ABAH dose has been determined in prior studies and results in ~40% attenuation of MPO activity *in vivo* (Forghani et al., 2012; 2014). To determine cell proliferation, the thymidine analog, 5-bromo-2'-deoxyuridine (BrdU, 50 mg/kg in 0.9% saline, i.p., Sigma-Aldrich, St. Louis, MO) was administered twice daily from day 3 to day 7 after focal ischemia, and sacrificed on day 7. Another group was injected with BrdU from day 14 to day 21 after tMCAO and sacrificed on day 21 for immunostaining (Kim et al., 2009). In addition, we also performed Ki67 staining as another means to detect proliferating cells (see below). A schematic diagram showing the treatment regimens is shown in Supplementary Fig. 1B & C.

Immunohistochemistry

After deep anesthesia, mice were transcardially perfused with ice-cold phosphate buffered saline (PBS, pH 7.4). Brain tissues were submerged in dry ice-pre-cooled isopentane (Sigma-Aldrich) and stored in a -80 ◦C freezer. Brains were cut into serial coronal sections (20

μm) with a cryostat (Microm International GmbH, Model: HM 505 E, Walldorf, Germany) and stored in a -80°C freezer. Sections were fixed with 4% paraformaldehyde (PFA) for 15 min and washed three times for 10 min with PBS 0.1M (pH7.4). BrdU staining was performed in 2N HCl for 30 min to denature DNA and then with 0.1M boric acid (pH. 8.5) for 10 min.

After that the sections were incubated with a blocking solutions containing 0.1% Triton-X and 5% normal goat serum in PBS for 1 h at room temperature. The following primary antibodies were used in the immunostaining: rat anti-BrdU (1:100, Accurate Chemicals, Westbury, NY, USA), rabbit anti-doublecortin (1:250, Abcam, Cambridge, MA, USA), mouse anti-Nestin (1:200, Abcam), mouse anti-glial fibrillary acidic protein (GFAP) (1:500, Covance, Inc. Nashville, TN, USA), rabbit anti-Ki67 (1:200, Millipore, Billerica, MA, USA), rabbit anti-brain-derived neurotrophic factor (BDNF, 1:200, Millipore), rabbit anti-pCREB (Ser 133) (1:200, Millipore), rabbit anti-acetylated H3 (AcH3, 1:200, Millipore), mouse anti-NeuN (1: 200, Millipore), anti-ionized calcium binding adaptor molecule 1 (Iba-1, for microglia/macrophage) (1:250, Wako Pure Chemical Industries, Ltd., Oska, Japan), rat anti-ED1 (CD68, for monocytes/macrophage, 1:200, Bio-Rad Lab., Inc., Hercules, California, USA), rabbit anti-matrix metalloproteinase-9 (MMP-9, 1:200, Abcam) and rabbit anti-CXC chemokine receptor-4 (CXCR4) (1:250, Abcam). Brain sections were incubated overnight with primary antibody at 4°C and rinsed with PBS 3 times. Brain tissues were incubated with the secondary antibodies in humidified chambers for 2 h at room temperature. Conjugated secondary antibodies were linked with anti-rat Alexa fluor 555 (1:1000, Invitrogen, Eugene, OR, USA**)**, anti-rabbit Alexa fluor 488 (1:500, Invitrogen), anti-rabbit FITC and anti-mouse FITC (1:200, Jackson Immuno Research Laboratories, West Grove, PA, USA) depending on the primary antibody. Brain sections were washed three times for 10 min with PBS, mounted on super frost slides with

Fluorescent Mounting Medium (Vector Laboratories, Inc., Burlingame, CA, USA) and coverslip. Negative controls performed same procedures without primary antibodies and showed no specific staining. For immunohistochemistry, at least 3 animals were used for BrdU, GFAP, Ki67, Nestin, AcH3, BDNF, pCREB, CXCR4 and MPO immunostaining on day 7 or 21 post stroke, respectively.

Quantitative analysis for immunostaining

Images were acquired by fluorescence microscopy using the 40× objective lens (Nikon, Nikon Eclipse 80i, Japan) and various neural stem cell markers were analyzed in the ipsilateral hemispheres. We also performed BrdU staining on the SVZ and striatum of the contralateral hemisphere as control. Measurements in the areas of the SVZ, anterior SVZ (aSVZ), striatum and parietal cortex were made using three to five sections per animal (each group, n=3-4 mice**).** In the SVZ, BrdU, GFAP and other labeled cells were examined along the lateral walls of the lateral ventricles, corresponding to coronal coordinates bregma -0.30 to bregma -1.2 mm (Supplementary Fig. 2A). In the DG, BrdU, GFAP-labeled cells were analyzed within the inner edge of the granule cell layer of the dentate gyrus corresponding to bregma -4.52 to bregma -3.14 (Supplementary Fig. 2B). Single labeling of $BrdU^+$ and double labeling of $BrdU^+/GFAP^+$, $BrdU^+/Nestin^+$, $BrdU^+/DCX^+$, $BrdU^+/BDNF^+$, $BrdU^+/p\text{-}CREB^+$, $BrdU^+/acetylated\ H3^+$(AcH3), and $BrdU^+/NeuN^+$ cells were investigated in the ischemic brains on day 7 or 21 after tMCAO.

Statistical analysis

The data were analyzed using the GraphPad Software (Prism 6, Graph Pad Inc., La Jolla, CA, USA). Data were shown as mean ± SEM and a *p*-value less than 0.05 was considered as statistically significant. Between two groups, we used the student's t test. For multiple comparisons, we performed one way-ANOVA followed by Bonferroni's *post-hoc* test. Pearson's

correlation was computed for BrdU and 8-point behavior scores by linear regression. The number of mice used for each group was calculated to achieve a power of 90% (30% difference in means and standard deviation of 15% based on our prior experience using this model (Forghani et al, 2014)), resulting in n = 3 per group.

RESULTS

MPO inhibtion increased cell proliferation in the SVZ and striatum after stroke

Vehicle-treated stroke mice showed reduced 8-point neurological test scores up to day 21 (Forghani et al., 2014). In contradistinction, ABAH-treated stroke mice showed significantly improved 8-point test scores compared to vehicle-treated stroke mice, persisting to day 21 ($p < 0.001$, n=12 in each group). As expected, sham-operated animals showed no functional impairment at all the time points. There was no significant difference between animal groups in the mean Laser Doppler flow (LDF) values during stroke induction (Supplementary Fig. 3, 11.6 ± 0.9 versus (vs.) 11.8 ± 0.9 in the vehicle (n=30) vs. ABAH (n=30); p= 0.90). Thus, similar to our previous findings (Forghani et al., 2014), MPO inhibition improved functional outcome on our battery of behavioral tests covering motor, sensory and reflex functions. While the dominant mechanism for the improvement is from direct inhibition of MPO activity, we wondered whether neurogenesis increased given emerging associations between neuroinflammation and neurogenesis (Tobin et al., 2014).

We first evaluated cell proliferation using BrdU and Ki67. We chose to detect both markers because BrdU detects the S phase in DNA synthesis but Ki67 is expressed in all phases of the cell cycle (G1, S, M and G2) except the resting stage (G_0) (Taupin, 2007). As expected, sham-treated mice brains contained only a few $BrdU^+$ cells (Fig. 1A (i), B & D), and vehicle-

treated ischemic mice showed a slightly increased number of $BrdU^+$ cells in the SVZ compared to that of sham control mice (Fig. 1B & D). However, MPO inhibition with ABAH markedly increased the number of $BrdU^+$ cells in the ipsilateral SVZ and striatum compared to vehicle-treated group on day 7 after stroke (Fig. 1. A & C). As expected, the number of $BrdU^+$ cells in the contralateral hemispheres of sham-operated, vehicle-treated, and ABAH-treated animals did not increase compared to that in the ipsilateral hemisphere of sham-operated animals (Fig. 1 A & C). Quantified results for $BrdU^+$ cells in the ipsilateral SVZ (Fig. 1B) confirmed the increase in ABAH (n=7) vs. vehicle (n=7) treated stroke animals (11 ± 0.8 (vehicle) vs. 66.7 ± 3.0 (ABAH) cells/high power field (HPF=40X); $p < 0.001$). Similar findings were found for the ipsilateral striatum (Fig. 1D, 38.3 ± 0.7 vs. 72.7 ± 7.8 cells/HPF, vehicle (n=3) vs. ABAH (n=3); $p < 0.001$). The number of $BrdU^+$ cells was also increased following ABAH treatment in the ipsilateral aSVZ and parietal cortex on day 7 after stroke, respectively (Fig. 2B &D. aSVZ; 11.14 ± 0.9 vs. 39.4 ± 13 cells/HPF, $p < 0.001$. Pcox; 35.7 ± 10.3 vs. 62.3 ± 1.9 cells/HPF, $p < 0.05$, vehicle (n=7) vs. ABAH (n=7). Interestingly, ABAH treatment increased cell proliferation in the ipsilateral SVZ even 21 days after stroke. (Supplementary Fig. 4, 9.0 ± 1.7 vs. 44 ± 6.0 cells/HPF, vehicle (n=3) vs. ABAH (n=3); $p < 0.001$). There were also increased $BrdU^+$ cells in the OB of ABAH-treated stroke mice compared to vehicle-treated stroke mice (10%, data not shown). Similarly, there were more $Ki67^+$ cells in the ipsilateral SVZ on days 7 and 21 in ABAH-treated mice compared to those in vehicle-treated animals, respectively (Fig. 1E (i &-ii). Quantified results showed that ABAH treatment significantly increased the number of $Ki67^+$ cells compared to vehicle-treated animals on day 7 after stroke (Fig. 1F, 10.7 ± 0.7 vs. 32.0 ± 4.2 cells/HPF, vehicle (n=3) vs. ABAH (n=3); $p < 0.01$). On day 21 after stroke, $Ki67^+$ cells remain elevated

after ABAH treatment (10.3 ± 2.8 vs. 30.0 ± 1.7 cells/HPF, vehicle (n=3) vs. ABAH (n=3); $p < 0.01$).

ABAH treatment increased neurogenesis in the ischemic brains.

Multipotent GFAP-expressing progenitors (Type B cells) function as neurogenic stem cells in SVZ or DG, and astrocyte-NSC generate transit-amplifying progenitors, which then differentiate to neuroblasts or neurons (Garcia et al., 2004). Ablation of dividing GFAP-expressing cells abolishes neuroblast and newborn cells in DG (Garcia et al., 2004). Therefore, we used GFAP (an astrocyte marker) colocalized with BrdU to identify NSCs. We found that ABAH treatment increased the number of $BrdU^+/GFAP^+$ cells in the SVZ compared to vehicle-treated mice on day 7 post ischemia (Fig. 3A(i), B(i)), indicating an increase in neural stem cells. Quantified analysis confirmed these effects in the ipsilateral SVZ after stroke (Fig. 3C; 1.0 ± 0.6 vs. 21.3 ± 2.3 cells/HPF, vehicle (n=3) vs. ABAH (n=3); $p < 0.001$). On day 21 after stroke, ABAH treatment also increased the number of $BrdU^+/GFAP^+$ cells compared to vehicle-treated mice (21%, data not shown) in the ischemic subgranular layer (SGL) of the dentate gyrus (DG).

We also investigated the effects of ABAH on the expression of Nestin, a marker for neuroprogenitors such as type1 and type 2a cells. On day 7 after ABAH treatment, the number of $BrdU^+/Nestin^+$ cells increased compared to vehicle-treated stroke mice in the ipsilateral striatum (Fig. 3A (ii) & B (ii)). Interestingly, ABAH treatment also increased the number of $Nestin^+$ cells that already moved to the striatum on day 7 after stroke Quantified results of $BrdU^+/Nestin^+$ cells are shown in Fig. 3D; 1.0 ± 3.5 vs. 6.7 ± 0.9 cells/HPF, vehicle (n=3) vs. ABAH (n=3); $p < 0.01$).

Doublecortin (DCX)-expressing immature neuronal cells are found in the adult brain after stroke (Brown et al., 2003; Ohab et al., 2006). Animals treated with ABAH showed an

JPET Fast Forward. Published on August 22, 2016 as DOI: 10.1124/jpet.116.235127
This article has not been copyedited and formatted. The final version may differ from this version.

increase in the number of BrdU-DCX double-positive cells compared to vehicle-treatment in the ipsilateral SVZ on day 7 after stroke (Fig. 3A (iii), 3B (iii), and 3E; 4.3 ± 0.9 vs. 35 ± 7.6 cells/HPF, vehicle (n=3) vs. ABAH (n=3); $p < 0.01$). Sham-treated mice brains showed only a few $GFAP^+$, $Nestin^+$, and DCX^+ cells in the ischemic hemisphere. Taken together, our results revealed that MPO inhibition enhanced neurogenesis and increased neural stem cells, neuroprogenitors, and neuroblast populations.

MPO inhibition increased BDNF, p-CREB, AcH3, CXCR4, and NeuN in the ischemic brain

Brain-derived neurotrophic factor (BDNF) is a mitogenic factor that promotes the migration of NSC, enhances SVZ neuronal progenitor cell proliferation, neurogenesis and behavioral recovery (Benrasis et al., 2001; Chiamello et al., 2007; Kim et al., 2009; Ploughman, 2009). We next assessed whether ABAH treatment affects BDNF expression on day 7 post stroke. We found more $BrdU^+/BDNF^+$ cells in the ABAH-treated mice compared to vehicle-treated mice in the ischemic SVZ after stroke, showing that MPO inhibition increases BDNF expression (Fig. 4A (i) & B (i)). Quantified data showed that the number of $BrdU^+/BDNF^+$ cells significantly increased in the ABAH-treated animals on day 7 after tMCAO (Fig. 4C, 3.0 ± 1.5 vs. 30 ± 5.8 cells/HPF, vehicle (n=3) vs. ABAH (n=3); $p < 0.01$).

c-AMP response-element-binding protein (CREB) (Ser 133) activation increases survival of ischemia-induced neuronal precursors (Zhu et al., 2004; Giachino et al., 2005). ABAH treatment significantly increased the number of $BrdU^+/p\text{-}CREB^+$ (Ser 133) cells in the ischemic SVZ compared to vehicle-treated mice on day 7 post ischemia (Fig. 4A (ii) & B(ii)). Quantified result of $BrdU^+/p\text{-}CREB^+$ (Ser 133) cells in the SVZ are shown in Fig. 4D (7.3 ± 2.7 vs. 39.7 ± 6.7 cells/HPF, vehicle (n=3) vs ABAH (n=3); $p < 0.01$). Similarly, on day 21 after stroke, ABAH treatment increased the number of $BrdU^+/p\text{-}CREB^+$ cells compared to vehicle-treated control

mice in the SVZ (29%, data not shown). Therefore, MPO inhibition increased key factors in neurogenesis in the BDNF-p-CREB signaling pathway.

An increase in histone acetylation is important for neuronal lineage progression of neural progenitor cells. We found that ABAH treatment increased the number of $BrdU^+/AcH3^+$ cells compared to vehicle-treated mice in the ipsilateral SVZ on day 7 post strokes. Most $BrdU^+$ cells colocalized with $AcH3^+$ cells in this region (Fig. 4A (iii), B (iii), and 4E; 7.7 ± 0.7 vs. 35 ± 4.0 cells/HPF, vehicle (n=3) vs. ABAH (n=3); $p < 0.001$).

CXCR4, a receptor of chemokine stromal cell-derived factor 1, is expressed in neuroprogenitors and migrating neuroblasts in the ischemic hemisphere. ABAH treatment increased $CXCR4^+$ cells in the ipsilateral SVZ compared with vehicle-treated animals on day 7 post stroke, suggesting that MPO inhibition may contribute to NSC/progenitors migration in the damaged brain cell homing and migration (Fig. 4F).

Next, we investigated whether ABAH treatment increases NeuN (a mature neuronal marker)-positive cells after stroke. Treatment with ABAH for 7 days markedly enhanced the number of $BrdU^+/NeuN^+$ cells in the ipsilateral aSVZ and SVZ compared to sham-operated or vehicle-treated control animals (Fig. 5A-E). Quantified results of $BrdU^+/NeuN^+$ cells in the ipsilateral aSVZ confirmed this finding. Interestingly, most of the $BrdU^+$ cells colocalized with $NeuN^+$ cells in the aSVZ of ABAH-treated mice. (Fig. 5C, 2.7 ± 0.3 vs. 26 ± 4.4 cells/HPF, vehicle (n=3) vs. ABAH (n=3); $p < 0.01$). In the aSVZ, ABAH treatment also significantly increased the number of $NeuN^+$ cells compared to vehicle-treated animals (7.0 ± 0.58 cells/HPF vehicle (n=3) vs. 26.3 ± 3.5 cells/HPF ABAH (n=3); $p < 0.01$). We confirmed similar effects in the ipsilateral SVZ (Fig. 5D). Quantified results of $BrdU^+/NeuN^+$ cells in the ipsilateral SVZ confirmed these observations (Fig. 5E, 2.0 ± 0.58 vs 13.3 ± 4.3 cells/HPF, vehicle (n=3) vs.

JPET Fast Forward. Published on August 22, 2016 as DOI: 10.1124/jpet.116.235127
This article has not been copyedited and formatted. The final version may differ from this version.

ABAH (n=3); $p < 0.05$). The number of $NeuN^+$ cells in the ipsilateral SVZ also increased with ABAH treatment (14.3 ± 1.9 vs. 23 ± 0.6 cells/HPF, vehicle (n=3) vs. ABAH (n=3); $p < 0.01$).

MPO inhibition decreased the number of inflammatory cells and MMP-9 in the ischemic brain

We next determined whether MPO inhibition affects inflammatory cell recruitment and inflammatory mediators such as MMP-9. Iba-1 is a marker for myeloid cells and has a role in microglia activation and phagocytosis (Fumagalli et al., 2015). Amoeboid-shaped and hypertrophic Iba-1^+ cells were mainly observed in the ipsilateral striatum. ABAH treatment markedly reduced the number of Iba-1^+ cells compared with vehicle-treated control (Fig. 6, day 7: 23.7 ± 1.7 vs. 10.3 ± 0.7 cells/HPF, vehicle (n=3) vs. ABAH (n=3); $p < 0.001$ and day 21: 13.3 ± 0.3 vs. 3.7 ± 0.7 cells/HPF, vehicle (n=3) vs. ABAH (n=3); $p < 0.001$). Additionally, we investigated the effects of ABAH treatment on the ED1 (CD68)-positive cells, a marker for monocytes/macrophages. $ED1^+$ cells were detected in the ischemic striatum, and these cells were decreased by ABAH treatment on day 7 after stroke (Fig. 6A (iii) & D, 29.3 ± 1.2 vs. 18.0 ± 0.6 cells/HPF, vehicle (n=3) vs. ABAH (n=3); $p < 0.001$).

Matrix metalloproteinases (MMPs) also play a crucial role in brain inflammation by increasing BBB permeability through destruction of extracellular matrix (Park et al., 2009). Neutrophil infiltration contributes to the increase matrix metalloproteinase-9 (MMP-9) in the ischemic brain (Justicia et al., 2003) in stroke patients (Lo et al., 2003). We found that post-ABAH administration MMP-9^+ cells decreased compared to those of vehicle-treated animals in the ipsilateral striatum on day 7 post-stroke (Fig. 6A (iv), j-l). Quantified result was shown in Fig. 6E (23.3 ± 3.8 vs. 9.0 ± 2.5 cells/HPF, vehicle (n=3) vs. ABAH (n=3); $p < 0.05$). Our findings

revealed that post-insult ABAH treatment decreased inflammatory cell recruitment and BBB disruption.

MPO$^{-/-}$ stroke mice show increased cell proliferation and improved functional recovery after stroke

Corroborating our hypothesis, MPO$^{-/-}$ stroke mice also showed increased number of BrdU^{+} cells in the vehicle-treated group in the ipsilateral SVZ and striatum (Fig. 7A & B). To further determine whether the observed results were specifically due to ABAH's effect on MPO, we gave MPO$^{-/-}$ mice either ABAH or saline. There was no significant difference between the treatment groups in MPO$^{-/-}$ mice in both the ipsilateral SVZ (Fig. 7C, 18.7 ± 3.7 vs. 19 ± 2.3 cells/HPF, vehicle (n=3) vs. ABAH (n=3); $p > 0.05$) and the striatum on day 7 after stroke (Fig. 6D, 22.3 ± 8.0 vs. 31.3 ± 2.8 cells/HPF, vehicle (n=3) vs. ABAH (n=3); $p > 0.05$). In contradistinction, in wild-type stroke mice there was marked increase in the number of BrdU^{+} cells after ABAH treatment in both the SVZ and striatum ($p < 0.001$).

Next, we investigated whether MPO$^{-/-}$ mice demonstrate improved functional recovery after stroke using the 8-point test. MPO$^{-/-}$ stroke mice given either ABAH or saline showed no neurobehavioral difference up to day 21 following cerebral ischemia (Fig. 8A). Furthermore, sham-induced wild type mice given saline or ABAH also demonstrated no neurobehavioral difference between the two groups (Fig. 8B). These results confirmed that ABAH treatment with MPO$^{-/-}$ mice does not have additional effects other than MPO inhibition, and the changes we observed with ABAH treatment in WT stroke mice were due to ABAH's effect on MPO.

We also performed correlational analysis between BrdU^{+} cells and 8-point scores on day 7 after stroke. We found that higher number of BrdU^{+} cells was correlated with better

neurological outcome ($r = 0.86$, $p < 0.001$, Fig. 8C), and ABAH-treated stroke animals had more proliferating cells and better neurological outcome.

DISCUSSION

We had previously shown that MPO inhibition or congenital absence both led to a large reduction in infarct size (Forghani et al, 2014). The present work reveals that inhibiting the inflammatory enzyme MPO with the specific irreversible inhibitor ABAH not only resulted in decreased inflammatory cell recruitment and inflammatory mediators, but also decreased promotes cell proliferation and NSC/progenitor migration, and enhances neuronal differentiation leading to increased neurogenesis in the ischemic SVZ, aSVZ, striatum and cortex. We found that MPO inhibition increased markers for neurogenesis, including $BrdU^+$, $GFAP^+$, Ki 67^+, $Nestin^+$, DCX^+, $BDNF^+$, p-$CREB^+$ (Ser133) and $AcH3^+$ cells in the ipsilateral SVZ, striatum and DG after ischemia, establishing an inverse relationship between MPO activity and neurogenesis. By treating ischemic $MPO^{-/-}$ mice with either ABAH or saline and finding no difference in the number of $BrdU^+$ cells or functional outcome, we confirmed that it was the absence or inhibition of MPO, rather than nonspecific effects of ABAH, that resulted in the observed effects on neurogenesis. Interestingly, MPO appears to be involved in all stages of neurogenesis. This is likely attributed to the presence of MPO even up to day 21 after stroke (Breckwoldt et al, 2008) that would continue to adversely affect neurogenesis when present.

BDNF is involved in neurogenesis, migration, maturation, and survival of newborn cells in the striatum after ischemic injury (Benraiss et al. 2001; Pencea et al., 2001). Additionally, BDNF-TrkB signaling cascade is a positive regulator of neurogenesis and oligodendrogenesis in the ipsilateral SVZ and DG, and can result in anti-inflammatory effects and contribute to

behavioral improvement after permanent MCAO in rats (Kim et al., 2009; Bath and Lee, 2010; Kim et al., 2014). Activation of CREB (Ser133) by phosphorylation also stimulates neurogenesis in the ischemic DG after focal ischemia in rodents (Zhu et al. 2004). Our results demonstrated that MPO inhibition increased BDNF-CREB signaling cascade, indicating MPO activity negatively affects this neurogenesis-signaling pathway. Elevated oxidative stress in stroke can reduce histone acetylation expression, important for gene regulation. Histone deacetylase (HDAC) inhibitors enhanced histone acetylation including acetylated H3 (AcH3) or acetylated H4 (AcH4) after stroke (Kim et al., 2007; Kim et al., 2009). HDAC inhibitors such as valproic acid and butyrate also can decrease MPO activity in LPS-induced lung injury (Ni et al., 2010; Ji et al., 2013). Indeed, we found MPO inhibition restored histone acetylation, known to result in more opened chromatin structure and induce NSC/progenitor production (Kim et al. 2009). In addition, we found that higher number of $BrdU^+$ cells correlated with better behavioral outcome, suggesting that improving neurogenesis is associated with neurological improvement.

While we found that MPO activity adversely impacts neurogenesis after stroke, how MPO activity exerts its effects on neurogenesis is likely complex and beyond the scope of this current study. Nonetheless, one can hypothesize that MPO activity increases inflammation that is detrimental to neurogenesis. In addition to direct cytotoxic effects of MPO activity, elevated MPO activity increases levels of ROS, MMP, inducible nitric oxide synthase (iNOS), and inflammatory cytokines (e.g., IL-1β, TNF-α) (Ekdahl et al., 2003; Monje et al., 2003; Cacci et al., 2008), creating an environment that is hostile to newborn cells. MPO inhibition can reduce these inflammatory mediators. Indeed, we found that MPO inhibition decreased MMP-9 levels in the infarct (Fig. 6E). Furthermore, we found that ABAH treatment decreased the number of inflammatory cells in the ischemic areas (Fig. 6), likely as a result of reduced inflammation.

JPET Fast Forward. Published on August 22, 2016 as DOI: 10.1124/jpet.116.235127
This article has not been copyedited and formatted. The final version may differ from this version.

Thus, these direct and indirect effects of MPO inhibition combine to provide an environment that is more friendly for neurogenesis in the ischemic brain.

NADPH oxidase (NOX) is an important pro-oxidant enzyme and triggers the generation of superoxide anion (O_2^-) and H_2O_2, which are major sources of ROS (Bedard and Krause 2007). The ablation of NOX2 in $gp91^{phox-/-}$ mice markedly reduced infarct size and inflammation compared to WT mice (Chen et al., 2009; Wang et al., 2013). Inhibition of NOX by apocynin treatment reduced ROS, neuroprotective effect and improves functional outcome in MCAO (Tang et al., 2007). Interestingly, neural progenitors use NOX derived H_2O_2 to maintain neurogenesis (Dickinson et al., 2011; Le Belle et al., 2011), showing that NOX has beneficial roles in ischemic injury. MPO acts downstream of NOX and unlike the membrane-bound NOX, MPO is secreted extracellularly where it can cause damage away from the source. NADPH oxidase deficiency leads to the often lethal chronic granulomatous disease (CGD) in human and CGD like-phenotype in mice (Nakano et al., 2008; Sorce and Krause 2009). On the other hand, MPO deficiency has not been found to significantly impact mortality (Kutter, 1998; Lanza, 1998; Kutter, 2000), making MPO a potential target for human translation. Neural stem cells and neural precursor cells can undergo asymmetric cell division and maintain NSC pools, allowing for damaged brain repair (Tobin et al., 2014). Thus, part of the beneficial effects of MPO inhibition may be from increased neurogenesis. While no clinically-approved drug is available to specifically inhibit MPO, several preclinical candidates are in development and one candidate has completed a phase IIa trial (Churg et al., 2012; Forbes LV et al., 2013; Ward J et al., 2013). Interestingly, we found that partial inhibition of MPO by ABAH led to a greater increase of $BrdU^+$ cells, up to ~70 cells (Fig. 1B). In contrast, congenital absence of MPO only increased $BrdU^+$ cells to ~20 cells (Fig. 7A-D). This suggests that congenital deletion of MPO is less

favorable to cell proliferation compared to pharmacological partial (~40% with ABAH) inhibition of MPO (Forghani et al., 2014). Indeed, several studies have found that MPO-deficient mice have altered immune responses, including increased nitric oxide and T-lymphocytes levels that may adversely affect neurogenesis (Brennan et al., 2001, Kumar et al., 2005). While we found increased neurogenesis associated with MPO inhibition, functional improvement with MPO inhibition was detected within 1 day after stroke (Forghani et al., 2014), suggesting that ABAH has neuroprotective effects prior to the onset of neurogenesis. We are currently also investigating this aspect of MPO inhibition. Taken together, improving our understanding of the actions of MPO and consequences of its inhibition in stroke, which resulted in improved functional recovery and neurogenesis, could spur further development of this new class of drugs to treat stroke patients.

CONCLUSION

Our findings indicate that MPO activity is inversely related to neurogenesis and possibly neurological outcome. MPO inhibition or deficiency in stroke, along with the associated effects on inflammation, creates an environment that stimulates important endogenous resources to promote many aspects of neurogenesis, including cell proliferation, differentiation, migration and newborn cell survival, providing evidence that links MPO-mediated inflammation with neurogenesis in stroke.

Authorship Contributions

Participated in research design: H.J.K., J.W.C., M.A.M.
Contributed new reagents or analytic tools: H.J.K., W.Y.
Conducted experiments: H.J.K., W.Y., J.Y.L., Y.Z., Y.W.
Performed data analysis: H.J.K., J.Y.L., J.W.C.
Wrote or contributed to the writing of the manuscript: H.J.K., J.W.C.

JPET Fast Forward. Published on August 22, 2016 as DOI: 10.1124/jpet.116.235127
This article has not been copyedited and formatted. The final version may differ from this version.

REFERENCES

Alvarez-Buylla A and Garcia-Verdugo JM (2002) Neurogenesis in adult subventricular zone. *J Neurosci* **22:** 629-634.

Arvidsson A, Collin T, Kirik D, Kokaia Z, and Lindvall O (2002) Neuronal replacement from endogenous precursors in the adult brain after stroke. *Nat Med* **8:** 963-970.

Bath KG and Lee FS (2010) Neurotrophic factor control of adult SVZ neurogenesis. *Dev Neurobiol* **70:**339-349.

Bedard K and Krause KH (2007) The NOX family of ROS-generating NADPH oxidases: physiology and pathophysiology. *Physiol Rev* **87:** 245-313.

Benraiss A, Chmielnicki E, Lerner K, Roh D, and Goldman SA (2001) Adenoviral brain-derived neurotrophic factor induces both neostriatal and olfactory neuronal recruitment from endogenous progenitor cells in the adult forebrain. *J Neurosci* **21:**6718-6731.

Breckwoldt MO, Chen JW, Stangenbergb L, Aikawab E, Rodriguezb E, Qiud S, Moskowitz MA, and Weissleder R (2008) Tracking the inflammatory response in stroke in vivo by sensing the enzyme myeloperoxidase. *Proc Natl Acad Sci USA.* **105:**18584-18589.

Brennan M, Gaur A, Pahuja A, Lusis AJ, and Reynolds WF (2001) Mice lacking myeloperoxidase are more susceptible to experimental autoimmune encephalomyelitis.

J Neuroimmunol **112:** 97-105.

Brown JP, Couillard-Després S, Cooper-Kuhn CM, Winkler J, Aigner L, and Kuhn HG (2003) Transient expression of doublecortin during adult neurogenesis. *J Comp Neurol* **467:**1-10.

Cacci E, Ajmone-Cat MA, Anelli T, Biagioni S, and Minghetti L (2008) In vitro neuronal and glial differentiation from embryonic or adult neural precursor cells are differently affected by chronic or acute activation of microglia. *Glia.* **56:**412-425.

Chamorro A and Hallenbeck J (2006) The harms and benefits of inflammatory and immune responses in vascular disease. *Stroke* **37:**291-293.

Chen H, Song YS, and Chan PH (2009) Inhibition of NADPH oxidase is neuroprotective after ischemia-reperfusion. *J Cereb Blood Flow Metab* **29:**1262-1272.

Chen JW, Breckwoldt MO, Aikawa E, Chiang G, and Weissleder R (2008) Myeloperoxidase-targeted imaging of active inflammatory lesions in murine experimental autoimmune encephalomyelitis. *Brain* **131:**1123-1133.

Chiaramello S, Dalmasso G, Bezin L, Marcel D, Jourdan F, Peretto P, Fasolo A, and De Marchis S (2007) BDNF/TrkB interaction regulates migration of SVZ precursor cells via PI3-K and MAP-K signaling pathway. *Eur J Neurosci* **26:**1780-1790.

Churg A, Marshall CV, Sin DD, Bolton S, Zhou S, Thain K, Cadogan EB, Maltby J, Soars MG, Mallinder PR, and Wright JL (2012) Late intervention with a myeloperoxidase inhibitor stops progression of experimental chronic obstructive pulmonary disease. *Am J Respir Crit Care Med* **185:**34-43.

Curtis MA, Kam M, Nannmark U, Anderson MF, Axell MZ, Wikkelso C, Holtas S, van Roon-Mom WM, Bjork-Eriksson T, Nordborg C, Frisen JF, Dragunow M, Faull RL, and Eriksson PS (2007) Human neuroblasts migrate to the olfactory bulb via a lateral ventricular extension. *Science.* **315:**1243-1249.

Dickinson BC, Peltier J, Stone D, Schaffer DV, and Chang CJ (2011) Nox2 redox signaling maintains essential cell populations in the brain. *Nat Chem Biol* **7:**106-112.

Ekdahl CT, Claasen JH, Bonde S, Kokaia Z, and Lindvall O (2003) Inflammation is detrimental for neurogenesis in adult brain. *Proc Natl Acad Sci USA.* **100:**13632-13637.

El Kebir D, Filep JG (2013). Modulation of neutrophil apoptosis and the resolution of Inflammation through β2 Integrins. Front Immunol 4:60. doi: 10.3389/fimmu.2013.00060. eCollection.

Forbes LV, Sjögren T, Auchère F, Jenkins DW, Thong B, Laughton D, Hemsley P, Pairaudeau G, Turner R, Eriksson H, Unitt JF, and Kettle AJ (2013) Potent reversible inhibition of myeloperoxidase by aromatic hydroxamates. *J Biol Chem* **288:**36636-33647.

Forghani R, Kim HJ, Wojtkiewicz GR, Bure L, Wu Y, Hayase M, Wei Y, Zheng Y, Moskowitz MA, and Chen JW (2014) Myeloperoxidase propagates damage and is a potential therapeutic target for subacute stroke. *J Cereb Blood Flow Metab* **35:** 485-493.

Forghani R, Wojktiewicz GR, Zhang Y, Seeburg D, Bautz BRM, Pulli B, Milewski AR, Atkinson WL, Iwamoto Y, Zhang ER, Etzrodt M, Rodriguez E, Robbins CS, Swirski FK, Weissleder R, and Chen JW (2012) Demyelinating disease: Myeloperoxidase as an imaging biomarker and therapeutic target. *Radiology* **263:**451-460.

Fumagalli S, Perego C, Pischiutta F, Zanier ER, De Simoni MG (2015) The ischemic environment drives microglia and macrophage function. Front Neurol. 6:81. doi: 10.3389/fneur.2015.00081. eCollection 2015.

Garcia AD, Doan NB, Imura T, Bush TG, and Sofroniew MV (2004) GFAP-expressing progenitors are the principal source of constitutive neurogenesis in adult mouse forebrain. *Nat Neurosci* **7:**1233-1241.

Giachino C, De Marchis S, Giampietro C, Parlato R, Perroteau I, Schutz G, Fasolo A, and Peretto P (2005) cAMP response element-creb binding protein regulates differentiation and survival of newborn neurons in the olfactory bulb. *J Neurosci* **25:**10105-10118.

Heinecke JW (2002) Tyrosyl radical production by myeloperoxidase: a phagocyte pathway for lipid peroxidation and dityrosine cross-linking of proteins. *Toxicology* **177:**11-22.

Iosif RE, Ahlenius H, Ekdahl CT, Darsalia V, Thored P, Jovinge S, Kokaia Z, and Lindvall O (2008) Suppression of stroke-induced progenitor proliferation in adult subventricular zone by tumor necrosis factor receptor 1. *J Cereb Blood Flow Metab* **28:**1574-1587.

Ji MH, Li GM, Jia M, Zhu SH, Gao DP, Fan YX, Wu J, and Yang JJ (2013) Valproic acid attenuates lipopolysaccharide-induced acute lung injury in mice. *Inflammation* **36:**1453-1459.

Jin K, Sun Y, Xie L, Peel A, Mao XO, Batteur S, and Greenberg DA (2003) Directed migration of neuronal precursors into the ischemic cerebral cortex and striatum. *Mol Cell Neurosci* **24:** 171-189.

Justicia C, Panés J, Solé S, Cervera A, Deulofeu R, Chamorro A, and Planas AM (2003) Neutrophil Infiltration Increases Matrix Metalloproteinase-9 in the ischemic brain after occlusion/reperfusion of the middle cerebral artery in rats. *J Cereb Blood Flow Metab* **23**: 1430-1440.

Kim HJ and Chuang DM (2014) HDAC inhibitors mitigate ischemia-induced oligodendrocyte damage: potential roles of oligodendrogenesis, VEGF, and anti-inflammation. *Am J Transl Res* **6:** 206-223.

Kim HJ, Leeds P, and Chuang DM (2009) The HDAC inhibitor, sodium butyrate, stimulates neurogenesis in the ischemic brain. *J Neurochem* **110:**1226-1240.

Kim HJ, Rowe M, Ren M, Hong JS, Chen PS, and Chuang DM (2007) HDAC inhibitors exhibit anti-inflammatory and neuroprotective effects in a rat permanent ischemic model of stroke: Multiple mechanisms of action. *J Pharmacol Exp Ther* **321:**892-901.

Klinke A, Nussbaum C, Kubala L, Friedrichs K, Rudolph TK, Rudolph V, Paust HJ, Schröder C, Benten D, Lau D, Szocs K, Furtmüller PG, Heeringa P, Sydow K, Duchstein HJ, Ehmke H, Schumacher U, Meinertz T, Sperandio M, and Baldus S (2011) Myeloperoxidase attracts neutrophils by physical forces**.** *Blood* **117:**1350-1358.

Kohman RA, Rhodes JS (2013) Neurogenesis, inflammation and behavior. *Brain Behav Immun* **27**: 22-32.

Kumar AP, Ryan C, Cordy V, and Reynolds WF (2005) Inducible nitric oxide synthase expression is inhibited by myeloperoxidase. *Nitric Oxide* **13:**42-53.

Kutter D (1998) Prevalence of myeloperoxidase deficiency: population studies using Bayer-Technicon automated hematology. *J Mol Med* **76:** 669-675.

Kutter D, Devaquet P, Vanderstocken G, Paulus JM, Marchal V, and Gothot A (2000) Consequences of total and subtotal myeloperoxidase deficiency: risk or benefit? *Acta Haematol* **104:**10-15.

Lanza F (1998) Clinical manifestation of myeloperoxidase deficiency. *J Mol Med* **76:** 676-681.

Lau D and Baldus S (2006) Myeloperoxidase and its contributory role in inflammatory vascular disease. *Pharmacol Ther* **111:**16-26.

Le Belle JE, Orozco NM, Paucar AA, Saxe JP, Mottahedeh J, Pyle AD, Wu H, and Komblum HI (2011) Proliferative neural stem cells have high endogenous ROS levels that regulate self-renewal and neurogenesis in PI3K/Akt-dependent manner. *Cell Stem Cell* **8:** 59-71.

Lo EH, Dalkara T, Moskowitz MA (2003) Mechanisms, challenges and opportunities in stroke. *Nature reviews Neurosci* **4**: 339-415.

Lo EH, Moskowitz MA, and Ladecola C (2010) The science of stroke: mechanisms of search of treatment. *Neuron* **67:**181-198.

Maki RM, Tyurin VA, Lyon RC, Hamilton RL, Dekosky ST, Kagan VE, and Reynolds WF (2009) Aberrant expression of myeloperoxidase in astrocytes promotes phospholipid oxidation and memory deficits in a mouse model of Alzheimer. *J Biol Chem* **284:**3158-3169.

Ming Gl and Song HJ (2011) Adult neurogenesis in the mammalian brain: significant answers and significant questions. *Neuron* **70:**687-702.

Monje ML, Toda H, and Palmer TD (2003) Inflammatory blockade restores adult hippocampal

neurogenesis. *Science* **302:**1760-1765.

Nakano Y, Longo-Guess CM, Bergstrom DE, Nauseef WM, Jones SM, and Bánfi B (2008) Mutation of the Cyba gene encoding p22phox causes vestibular and immune defects in mice. *J Clin Invest* **118:**1176-1185.

Ni YF, Wang J, Yan XL, Tian F, Zhao JB, Wang YJ, and Jiang T (2010) Histone deacetylase inhibitor, butyrate, attenuates lipopolysaccharide-induced acute lung injury in mice**.** *Respir Res* **11:1-8.** 11:33. doi: 10.1186/1465-9921-11-33.

Nussbaum C, Klinke A, Adam M, Baldus S, and Sperandio M (2013) Myeloperoxidase: a leukocyte-derived protagonist of inflammation and cardiovascular disease. *Antioxid Redox Signal* **18:** 692-713.

Ohab JJ, Flemings BA, and Carmichael ST (2006) A neurovascular niche for neurogenesis after stroke. *J Neurosci* **26:**13007-13016.

Park KP, Rosell A, Foerch C, Xing C, Kim WJ, Lee S, Opdenakker G, Furie KL, Lo EH (2009) Plasma and brain matrix metalloproteinase-9 after acute focal cerebral ischemia in rats. *Stroke* 40: 2836-2842.

Pencea V, Bingaman KD, Wiegand SJ, and Luskin MB (2001) Infusion of brain-derived neurothophic factor into the lateral ventricle of the adult rat leads to new neurons in the parenchyma of the striatum, septum, thalamus, and hypothalamus. *J Neurosci* **21:**6706-6717.

Ploughman M, Windle V, MacLellan CL, White N, Dorė JJ, and Corbett D (2009) Brain-derived neurotrophic factor contributes to recovery of skilled reaching after focal ischemia in rats. *Stroke* **40:**1490-1495.

Sorce S and Krause KH (2009) NOX Enzymes in the Central Nervous System: From Signaling to Disease. *Antioxid Redox Signal* **11:** 2481-2504.

Tang LL, Ye K, Yang XF, and Zheng JS (2007) Apocynin attenuates cerebral infarction after transient focal ischaemia in rats. *J Int Med Res* **35:**517-22.

Taupin P (2007) BrdU immunohistochemistry for studying adult neurogenesis: paradigms, pitfalls, limitations, and validation. *Brain Res Rev* **53:**198-214.

Thored P, Arvidsson A, Cacci E, Ahlenius H, Kallur T, Darsalia V, Ekdahl CT, Kokaia Z, and Lindvall O (2006) Persistent production of neurons from adult brain stem cells during recovery after stroke. *Stem Cells* **24:**739-747.

Tobin MK, Bonds JA, Minshall RD, Pelligrino DA, Testai FD, and Lazarov O (2014) Neurogenesis and inflammation after ischemic stroke: what is known and where we go from here. *J Cereb Blood Flow Metab* **34:**1573-84.

Wang Q, Tang XN, and Yenari MA (2007) The inflammatory response in stroke. *J*

Neuroimmunol **184:** 53-68.

Wang Z, Wei X, Liu Kang, Zhang X, Yang F, Zhang H, He Y, Zhu T, Li F, Shi W, Zhang Y, Xu H, Liu J, and Yi F (2013) NOX2 deficiency ameliorates cerebral injury through reduction of complexin II-mediated glutamate excitotoxicity in experimental stroke. *Free Radic Biol Med* **65:** 942-951.

Ward J, Spath SN, Pabst B, Carpino PA, Ruggeri RB, Xing G, Speers AE, Cravatt BF, and Ahn K (2013) Mechanistic characterization of a 2-thioxanthine myeloperoxidase inhibitor and selectivity assessment utilizing click chemistry-activity-based protein profiling. *Biochemistry*. **52:** 9187-9201.

Yamashita T, Ninomiya M, Hernández Acosta P, García-Verdugo JM, Sunabori T, Sakaguchi M, Adachi K, Kojima T, Hirota Y, Kawase T, Araki N, Abe K, Okano H, and Sawamoto K (2006) Subventricular zone-derived neuroblasts migrate and differentiate into mature neurons in the post-stroke adult striatum. *J Neurosci* **26:** 6627-6636.

Zhang R, Brennan ML, Shen Z, Macpherson JC, Schmitt D, Molenda CE, and Hazen SL (2002) Myeloperoxidase functions as a major enzymatic catalyst for initiation of lipid peroxidation at sites of inflammation. *J Biol Chem* **277:** 46116-46122.

Zhang RL, Tourneau YL, Greeg SR, Wang Y, Toh Y, Robin AM, Zhang ZG, and Michael C (2007) Neuroblast division during migration toward the ischemic striatum: A study of dynamic

migratory and proliferative characteristics of neuroblast from the subventricular zone. *J Neurosci* **27:** 3157-3162.

Zhang R, Zhang Z, Wang L, Wang Y, Gousev A, Zhang L, Ho KL, Morshead C, and Chopp M (2004) Activated neural stem cells contribute to stroke-induced neurogenesis and neuroblast migration toward the infarct boundary in adult rats. *J Cereb Blood Flow Metab* **24:**441-448.

Zhao C, Deng W, and Gage FH (2008) Mechanisms and functional implications of adult neurogenesis. *Cell* **132:**645-660.

Zhu DY, Lau L, Liu SH, Wei JS, and Lu YM (2004) Activation of cAMP-response-element-binding protein (CREB) after focal cerebral ischemia stimulates neurogenesis in the adult dentate gyrus. *Proc Natl Acad Sci USA* **101:**9453-9457.

Footnote: This study was supported by the National Institute of Health [R01 NS070835 and R01 NS0721267].

JPET Fast Forward. Published on August 22, 2016 as DOI: 10.1124/jpet.116.235127
This article has not been copyedited and formatted. The final version may differ from this version.

Figures Legends

Fig. 1. MPO inhibition increased cell proliferation in the ischemic brain on day 7 after tMCAO. (A) BrdU staining in the SVZ in sham, vehicle-treated, and ABAH-treated tMCAO mice. $BrdU^+$ (red), $DAPI^+$ (blue), Merge ($BrdU^+$/$DAPI^+$). LV: lateral ventricle, SVZ: subventricluar zone, Contra = contralateral hemispheres. Arrows identify BrdU-positive cells. (B) Quantification of (A). Sham, vehicle- and ABAH-treated mice (n=7 in each group). (C) BrdU staining in the ipsilateral striatum in sham, vehicle-treated and ABAH-treated tMCAO mice. Contra = contralateral hemispheres. (D) Quantification of (C). Sham, vehicle- and ABAH-treated mice (n=3 in each group). (E) Ki67 staining in the ipsilateral SVZ in sham, vehicle-treated, and ABAH-treated mice on day 7 or 21 day after stroke. $BrdU^+$ (red), $Ki67^+$ (green), $DAPI^+$ (blue). Arrows identify Ki67-positive cells. Magnification, ×40. Scale bar, 50 μm. In the merged images, arrowheads indicate cells with co-localized expression of BrdU and Ki67. Scale bar, 25 μm. (F) Quantification of (E). Sham, vehicle- and ABAH-treated mice (n=3 in each group). Data are mean ± SEM. ANOVA followed by Bonferroni's *post-hoc* test. * $p < 0.05$, ** $p < 0.01$, *** $p < 0.001$.

Fig. 2. MPO inhibition increased cell proliferation in the ischemic aSVZ on day 7 after tMCAO. (A) BrdU staining in the ipsilateral aSVZ in sham, vehicle-treated, and ABAH-treated tMCAO mice. $BrdU^+$ (red), $DAPI^+$ (blue). Merge ($BrdU^+$/$DAPI^+$). LV: lateral ventricle, aSVZ: anterior subventricluar zone. Arrows identify BrdU-positive cells. (B) Quantification of (A). Sham, vehicle- and ABAH-treated mice (n=7 in each group). (C) BrdU staining in the ipsilateral parietal cortex in sham, vehicle-treated and ABAH-treated tMCAO mice. (D) Quantification of (C). Sham, vehicle- and ABAH-treated mice (n=3 in each group). Magnification, ×40. Scale bar,

50 μm. Data analyzed from 3 animals per group. Data are mean ± SEM. ANOVA followed by Bonferroni's *post-hoc* test. * $p < 0.05$, *** $p < 0.001$, ns: no significant.

Fig. 3. ABAH treatment increased neurogenesis on day 7 after stroke.

(A) ABAH treatment markedly increased 5-bromo-2'deoxyuridine (BrdU) labeling with increased expression of glial fibrillary acidic protein (GFAP), Nestin, and doublecortin (DCX) in the ipsilateral subventricular zone (SVZ) or striatum (Str) compared with saline-treated mice. (i) $BrdU^+$(red)/$GFAP^+$(green)/$DAPI^+$ (blue). (ii) $BrdU^+$ (red)/$Nestin^+$(green)/$DAPI^+$(blue). (iii) $BrdU^+$(red)/DCX^+(green)/$DAPI^+$(blue). Images are representative from 3-4 mice in each group. Magnification, ×60 (GFAP), Scale bar, 50 μm. Magnification, ×40 (BrdU, Nestin, DCX). Scale bar, 50 μm. (B) High-magnification images of the boxed areas in (A). $BrdU^+$(red), $GFAP^+$, $Nestin^+$, DCX^+ (green) and $DAPI^+$ (blue). (i, ii). Scale bar, 50 μm. (iii) Scale bar, 25 μm. (C) Quantification of $BrdU^+/GFAP^+$ cells in the ipsilateral SVZ of sham (n=3), vehicle- (n=3) and ABAH-treated (n=3) tMCAO mice. (D) Quantification of $BrdU^+/Nestin^+$ cells in the ipsilateral striatum of sham (n=3), vehicle- (n=3) and ABAH-treated (n=3) tMCAO mice. (E) Quantification of $BrdU^+/DCX^+$ cells in the ipsilateral SVZ of sham (n=3), vehicle- (n=3) and ABAH-treated (n=3) tMCAO mice. Data are mean ± SEM; ** $p < 0.01$, *** $p < 0.001$.

Fig. 4. ABAH treatment increased BDNF, p-CREB, Acetylated H3, and CXCR4-positive immunostaining in the SVZ on days 7 after tMCAO.

(A) Immunostaining for BDNF, p-CREB, and AcH3. $BrdU^+$ (red), $DAPI^+$ (blue). (i) $BDNF^+$ (green). (ii) p-$CREB^+$ (green). (iii) $AcH3^+$ (green). Magnification, ×40. Scale bar, 50 μm. (B) High-magnification images of the boxed areas in (A) from the ABAH treated group. Arrowheads

identify cells with co-localized expression. (i) Scale bar, 50 μm. (ii) Sclae bar, 30 μm. (iii) Sclae bar, 40 μm. (C) Quantification of $BrdU^+/BDNF^+$ cells. Sham, vehicle- and ABAH-treated mice (n=3 in each group). (D) Quantification of $BrdU^+/p\text{-}CREB^+$ cells. Sham, vehicle- and ABAH-treated mice (n=3 in each group). (E) Quantification of $BrdU^+/AcH3^+$ cells. Sham, vehicle- and ABAH-treated mice (n=3 in each group). Data are mean ± SEM; ** $p < 0.01$, *** $p < 0.001$. (F) (i) Immunostaining for chemokine receptor 4 (CXCR4) in the ipsilateral SVZ on day 7 after stroke. (ii) High-magnification images of the boxed areas in (i) ABAH-treated group. CXCR4 (green), DAPI (blue). Arrows indicate $CXCR4^+$ cells. Scale bar, 25 μm. LV, lateral ventricle; SVZ, subventricular zone.

Fig. 5. ABAH treatment increased the number of $BrdU^+/NeuN^+$ cells in the aSVZ and SVZ on day 7 after tMCAO mice. (A) Immunostaining of $BrdU^+/NeuN^+$ cells in the ipsilateral aSVZ in sham, vehicle-treated, and ABAH-treated tMCAO mice. Images are representative from 3-4 mice in each group. Magnification, ×40. Scale bar, 50 μm. (B) High-magnification images of the boxed areas in ABAH-treated mice. $BrdU^+$ (red), $NeuN^+$(green) and $DAPI^+$ (blue). Arrowheads indicate cells with co-localized expression. (C) Quantification of (A). Sham, vehicle- and ABAH-treated mice (n=3 in each group). (D) Immunostaining of $BrdU^+/NeuN^+$ cells in the ipsilateral SVZ (top) and contralateral SVZ (bottom) in sham, vehicle-treated, and ABAH-treated tMCAO mice, respectively. (E) Quantification of (D) SVZ in $BrdU^+/NeuN^+$ colocalization data. Sham, vehicle- and ABAH-treated mice (n=3 in each group). Data are mean ± SEM; * $p < 0.05$, ** $p < 0.01$.

JPET Fast Forward. Published on August 22, 2016 as DOI: 10.1124/jpet.116.235127
This article has not been copyedited and formatted. The final version may differ from this version.

Fig. 6. Post-insult ABAH treatment decreased the number of Iba-1$^+$, ED1$^+$ and MMP-9$^+$ cells on day 7 or day 21 after stroke. (A) (i) Immunostaining for Iba-1$^+$ cells on day 7 after stroke. Striatum; (a) sham, Iba-1$^+$ (green), (b) vehicle (c) ABAH. (ii) day 21 striatum; (d) sham, Iba-1$^+$ (green), (e) vehicle, (f) ABAH. Arrows show Iba-1$^+$ cells. (iii)-(iv). Immunostaining for ED1$^+$ and MMP-9$^+$ cells. Striatum, (g) sham, ED1$^+$ (green) cells. (h) vehicle (i) ABAH. Arrows identify ED1$^+$ cells. Striatum, (j) sham, MMP-9$^+$ (green). (k) vehicle, (l) ABAH. Arrows identify MMP-9$^+$ cells. (B & C) Quantification of Iba-1$^+$ cells in the ispilateral striatum on day 7 and 21 after stroke, respectively. (D &E) Quantification of ED1$^+$ cells and MMP-9 $^+$ cells in the ipsilateral striatum on day 7 after stroke, respectively. Data are mean ± SEM; * $p < 0.05$, ** $p < 0.01$, *** $p < 0.001$. n = 3 mice per group. Magnification, ×40. Scale bar, 50 μm.

Fig. 7. ABAH does not alter cell proliferation or neurobehavioral outcome in MPO$^{-/-}$ mice. (A) Stroke in MPO$^{-/-}$ mice increased cell proliferation compared to that of sham mice. Note that ABAH treatment in MPO$^{-/-}$ mice did not alter cell proliferation in the SVZ. Arrows indicate BrdU$^+$ cells. BrdU$^+$ (red), DAPI$^+$ (blue), and Merge (BrdU$^+$/DAPI$^+$). Sham, vehicle- and ABAH-treated mice (n=3 in each group). (B) Similar findings were found in the ipsilateral striatum in MPO $^{-/-}$ mice. Str: striatum. Arrows show BrdU$^+$ cells. (Sham, vehicle- and ABAH-treated mice (n=3 in each group). Magnification, ×40. Scale bar, 50 μm. ns = not significant. (C) Quantified result of BrdU-positive cells in the ipsilateral SVZ of MPO$^{-/-}$ mice and WT mice from Fig.1B. & Fig. 6A. Sham (WT): n=3, vehicle (WT): n=3, ABAH (WT): n=3; Sham (MPO$^{-/-}$): n=3; vehicle (MPO$^{-/-}$): n=3; ABAH (MPO$^{-/-}$): n=3). Data are mean ± SEM. ANOVA followed by Bonferroni's *post-hoc* test. * $p < 0.05$, *** $p < 0.001$, ns; no significant, between indicated groups. SVZ: anterior subventricluar zone. (D). Quantified result of BrdU-positive cells in the ipsilateral striatum of Fig.1D & Fig. 6B. Sham (WT): n=3, vehicle (WT): n=3, ABAH (WT): n=3, Sham

($MPO^{-/-}$): n=3, vehicle ($MPO^{-/-}$): n=3; ABAH ($MPO^{-/-}$): n=3). Data are mean ± SEM. ANOVA followed by Bonferroni's *post-hoc* test. *** $p < 0.001$, ns; no significant , between indicated groups.

Fig. 8. $MPO^{-/-}$ mice showed beneficial effect in functional outcome and sham-operated mice no effect on behavioral function between groups. (A) $MPO^{-/-}$ mice demonstrated improved 8-point neurological scores compared to vehicle-treated WT mice after stroke (compare to Supplementary Fig. 3A), and ABAH administration did not have any effect in $MPO^{-/-}$ mice. (B) Sham mice also showed no difference in the neurological scores with ABAH or vehicle treatment. Experimental conditions are the same as in Supplementary Fig. 3A. (C) Correlational analysis between $BrdU^{+}$ cell numbers and ABAH-treated 8-point behavioral score test on day 7 after stroke (n=14). Circles: vehicle-treated mice, triangles: ABAH-treated mice. r = 0.86, $p < 0.001$.

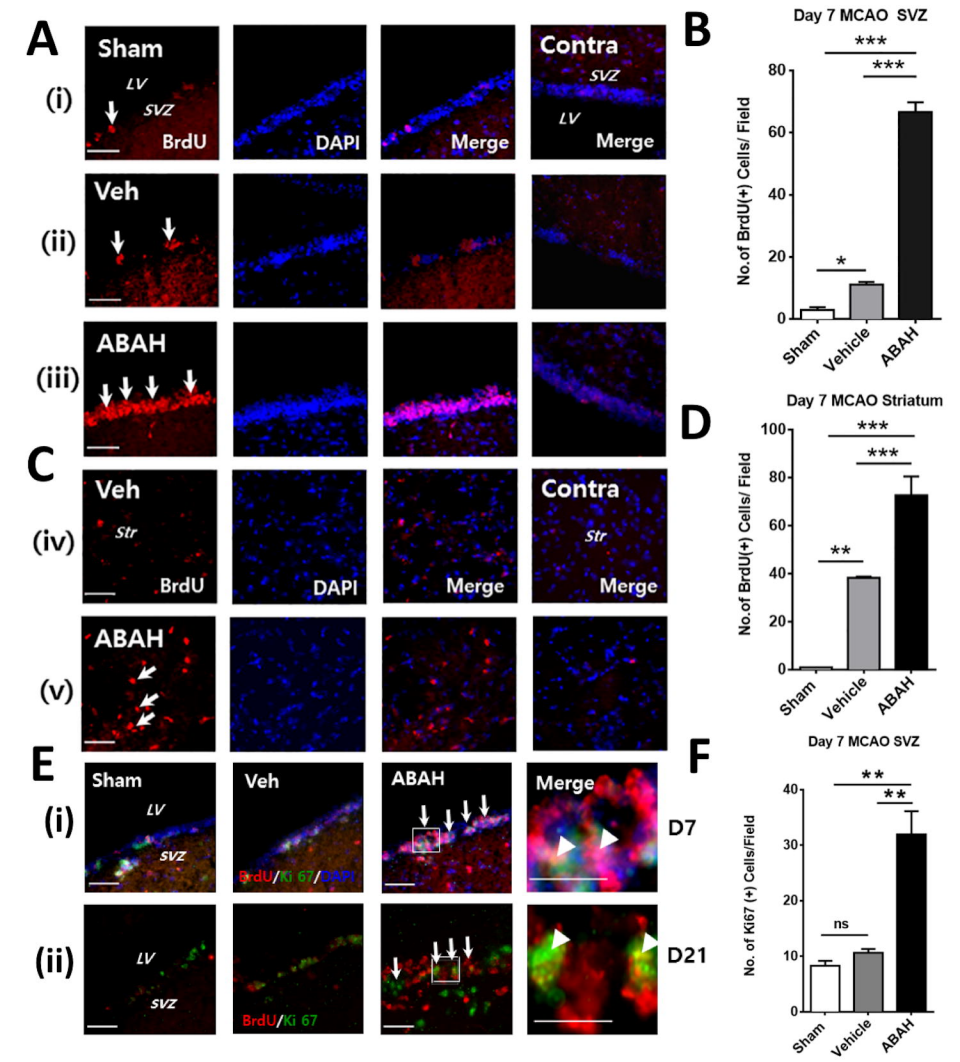
A
Sham
LV
SVZ
BrdU
DAPI
Merge
Contra
SVZ
LV
Merge
(i)
Veh
(ii)
ABAH
(iii)
B
Day 7 MCAO SVZ
No.of BrdU(+) Cells/ Field
Sham
Vehicle
ABAH
C
Veh
Str
BrdU
DAPI
Merge
Contra
Str
Merge
(iv)
ABAH
(v)
D
Day 7 MCAO Striatum
No.of BrdU(+) Cells/ Field
Sham
Vehicle
ABAH
E
Sham
LV
SVZ
Veh
ABAH
Merge
(i)
BrdU/Ki 67/DAPI
D7
(ii)
LV
SVZ
BrdU/Ki 67
D21
F
Day 7 MCAO SVZ
No. of Ki67 (+) Cells/Field
ns
Sham
Vehicle
ABAH

Figure 1

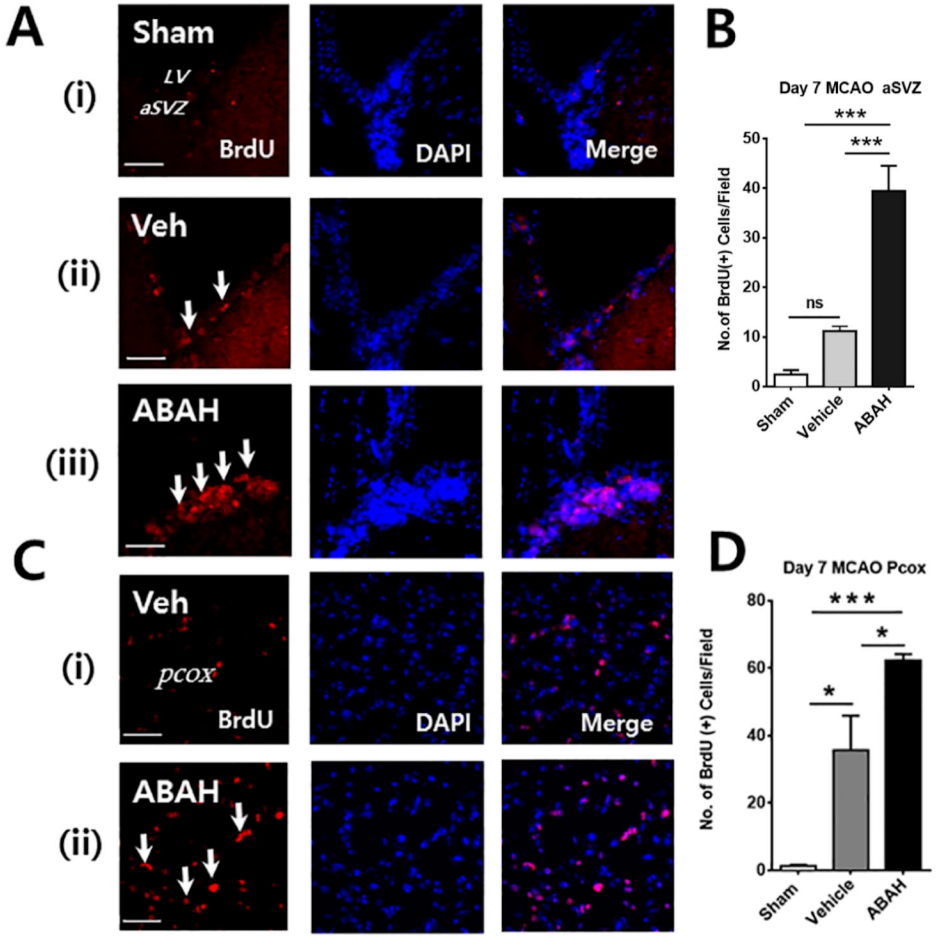
A
Sham
LV
aSVZ
BrdU
DAPI
Merge
(i)
Veh
(ii)
ABAH
(iii)
B
Day 7 MCAO aSVZ
***
***
ns
No.of BrdU(+) Cells/Field
50
40
30
20
10
0
Sham
Vehicle
ABAH
C
Veh
pcox
(i)
BrdU
DAPI
Merge
ABAH
(ii)
D
Day 7 MCAO Pcox
***
*
*
No. of BrdU (+) Cells/Field
80
60
40
20
0
Sham
Vehicle
ABAH

Figure 2

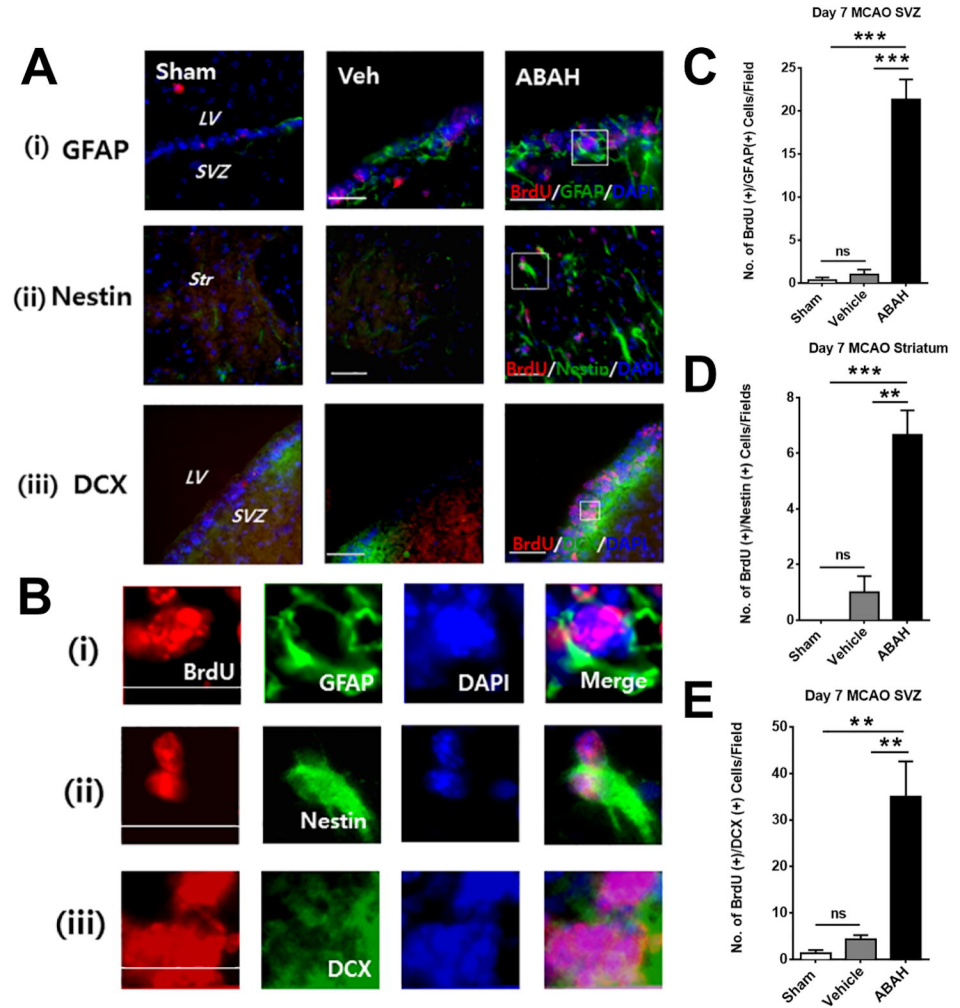
A
Sham
Veh
ABAH
(i) GFAP
LV
SVZ
BrdU/GFAP/DAPI
(ii) Nestin
Str
BrdU/Nestin/DAPI
(iii) DCX
LV
SVZ
BrdU/DCX/DAPI
B
(i)
BrdU
GFAP
DAPI
Merge
(ii)
Nestin
(iii)
DCX
C
Day 7 MCAO SVZ
***
***
No. of BrdU (+)/GFAP(+) Cells/Field
ns
Sham
Vehicle
ABAH
D
Day 7 MCAO Striatum
***
**
No. of BrdU (+)/Nestin (+) Cells/Fields
ns
Sham
Vehicle
ABAH
E
Day 7 MCAO SVZ
**
**
No. of BrdU (+)/DCX (+) Cells/Field
ns
Sham
Vehicle
ABAH

Figure 3

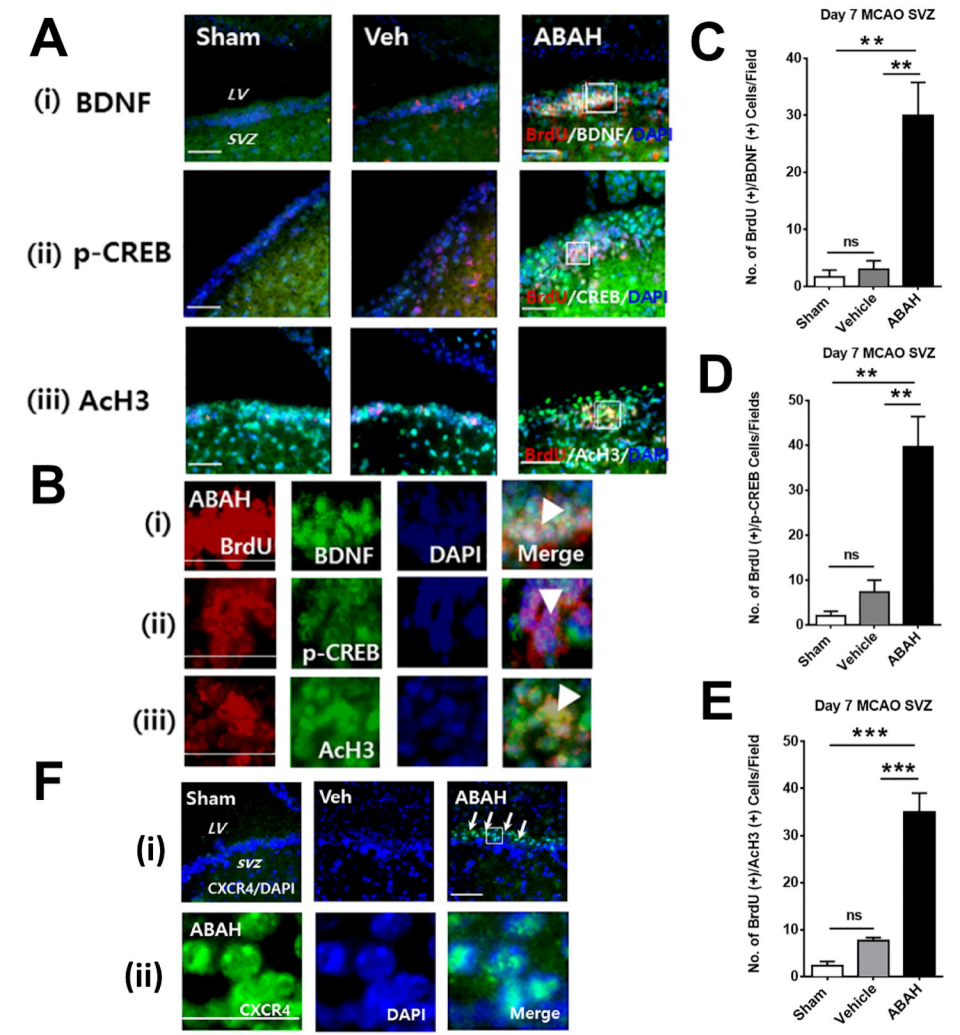
A
Sham
Veh
ABAH
(i) BDNF
LV
SVZ
BrdU/BDNF/DAPI
(ii) p-CREB
BrdU/CREB/DAPI
(iii) AcH3
BrdU/AcH3/DAPI
B
ABAH
BrdU
BDNF
DAPI
Merge
(i)
(ii)
p-CREB
(iii)
AcH3
F
Sham
Veh
ABAH
(i)
LV
SVZ
CXCR4/DAPI
ABAH
(ii)
CXCR4
DAPI
Merge
C
Day 7 MCAO SVZ
No. of BrdU (+)/BDNF (+) Cells/Field
**
**
ns
Sham
Vehicle
ABAH
D
Day 7 MCAO SVZ
No. of BrdU (+)/p-CREB Cells/Fields
**
**
ns
Sham
Vehicle
ABAH
E
Day 7 MCAO SVZ
No. of BrdU (+)/AcH3 (+) Cells/Field
***
***
ns
Sham
Vehicle
ABAH

Figure 4

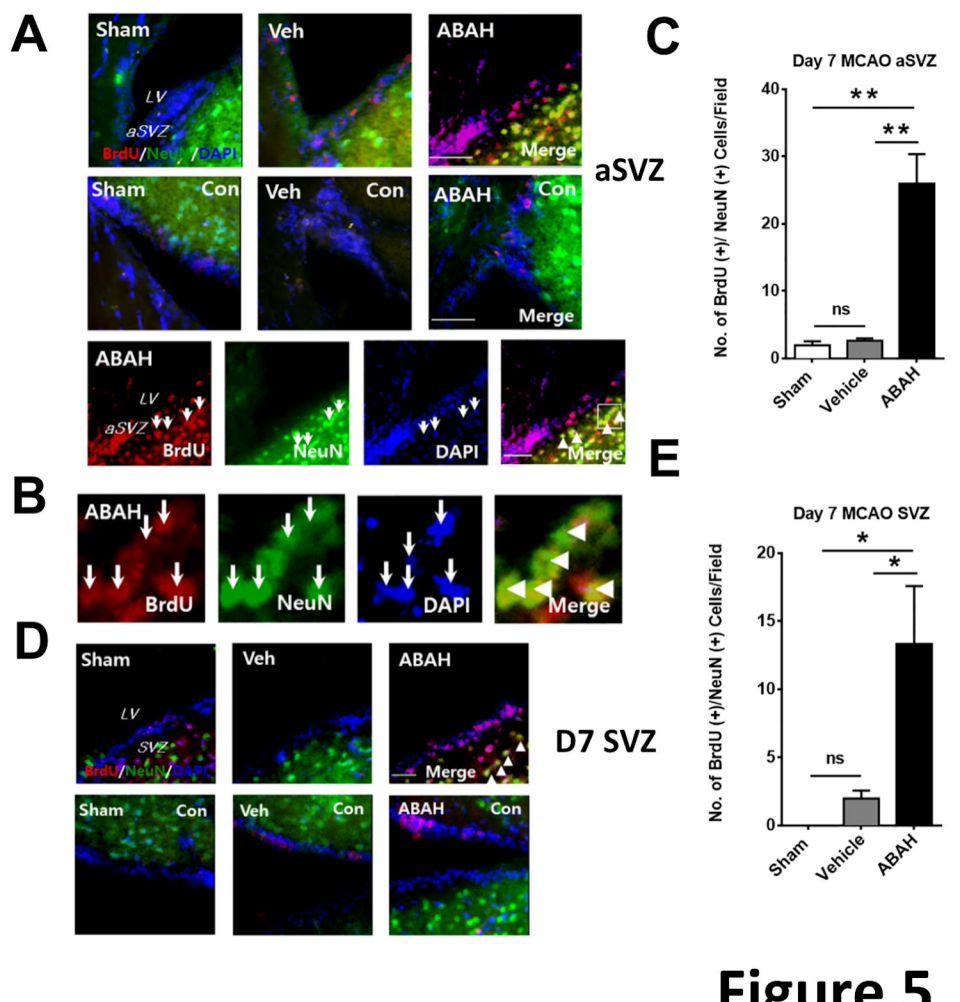
A
Sham
Veh
ABAH
LV
aSVZ
BrdU/NeuN/DAPI
Merge
aSVZ
Sham Con
Veh Con
ABAH Con
Merge
ABAH
LV
aSVZ
BrdU
NeuN
DAPI
Merge
B
ABAH
BrdU
NeuN
DAPI
Merge
D
Sham
Veh
ABAH
LV
SVZ
BrdU/NeuN/DAPI
Merge
D7 SVZ
Sham Con
Veh Con
ABAH Con
C
Day 7 MCAO aSVZ
No. of BrdU (+)/ NeuN (+) Cells/Field
40
30
20
10
0
**
**
ns
Sham
Vehicle
ABAH
E
Day 7 MCAO SVZ
No. of BrdU (+)/NeuN (+) Cells/Field
20
15
10
5
0
*
*
ns
Sham
Vehicle
ABAH

Figure 5

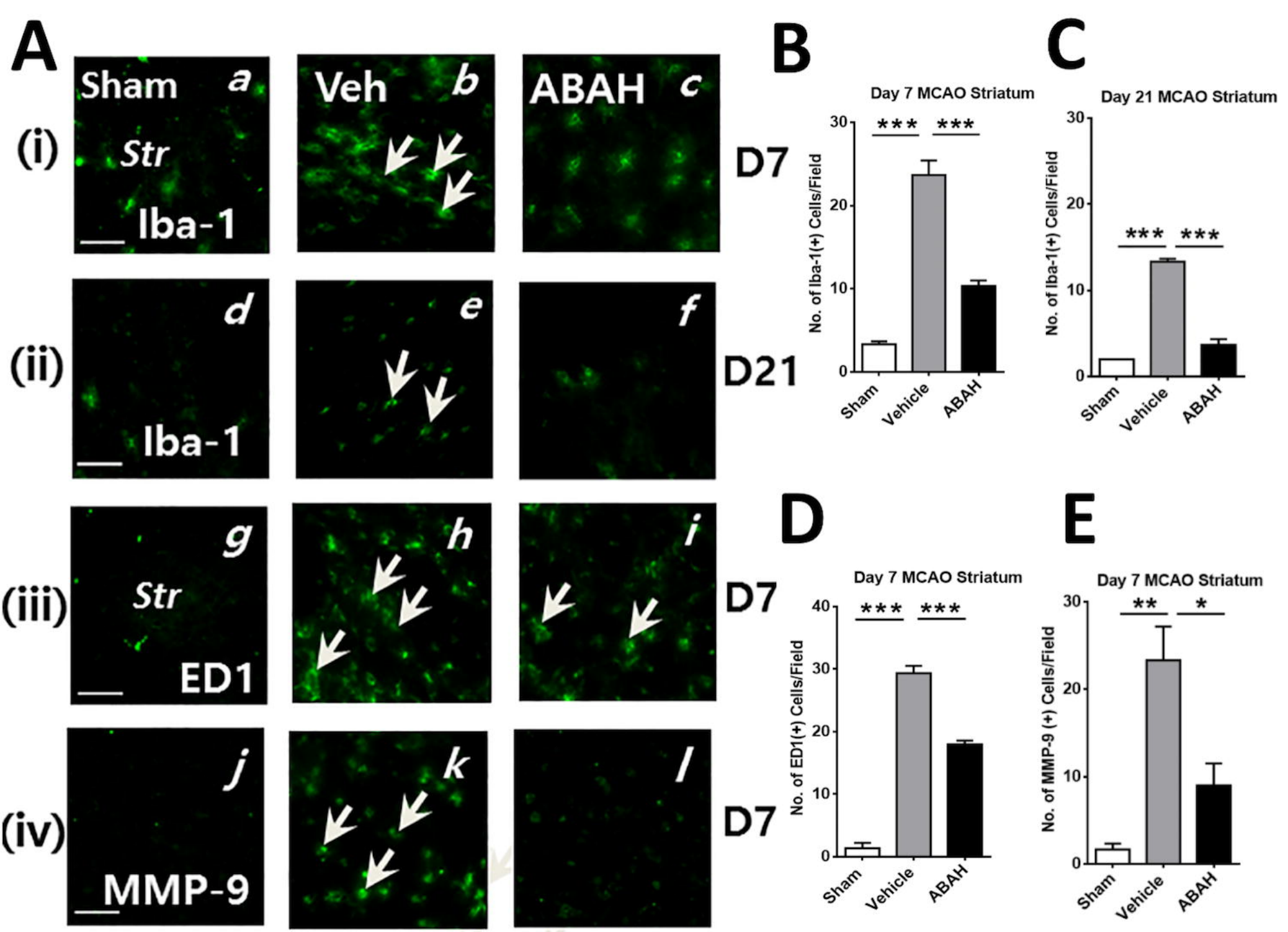
A
Sham
a
Veh
b
ABAH
c
(i)
Str
Iba-1
D7
d
e
f
(ii)
Iba-1
D21
g
h
i
(iii)
Str
ED1
D7
j
k
l
(iv)
MMP-9
D7
B
Day 7 MCAO Striatum
No. of Iba-1(+) Cells/Field
***
***
Sham
Vehicle
ABAH
C
Day 21 MCAO Striatum
No. of Iba-1(+) Cells/Field
***
***
Sham
Vehicle
ABAH
D
Day 7 MCAO Striatum
No. of ED1(+) Cells/Field
***
***
Sham
Vehicle
ABAH
E
Day 7 MCAO Striatum
No. of MMP-9 (+) Cells/Field
**
*
Sham
Vehicle
ABAH

Figure 6

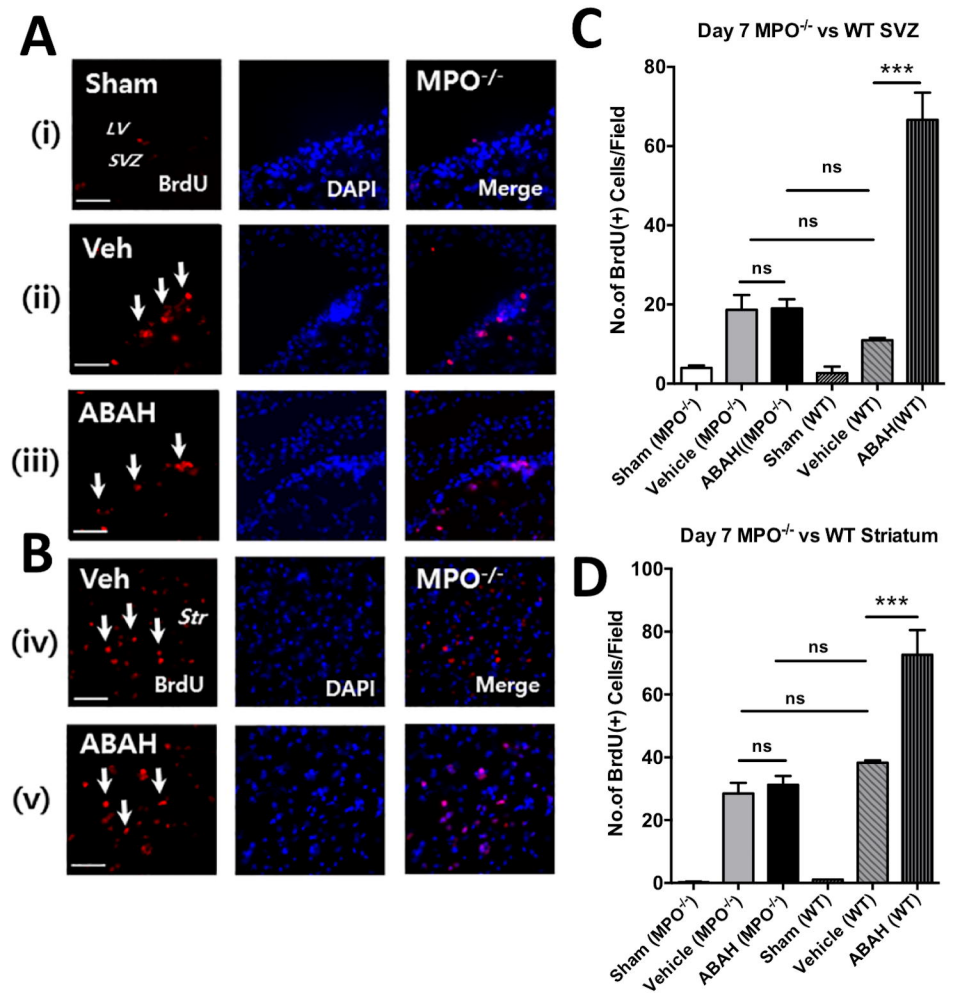
A
Sham
LV
SVZ
BrdU
DAPI
MPO-/-
Merge
(i)
Veh
(ii)
ABAH
(iii)
B
Veh
Str
BrdU
(iv)
DAPI
MPO-/-
Merge
ABAH
(v)
C
Day 7 MPO-/- vs WT SVZ
No.of BrdU(+) Cells/Field
80
60
40
20
0
***
ns
ns
ns
Sham (MPO-/-)
Vehicle (MPO-/-)
ABAH(MPO-/-)
Sham (WT)
Vehicle (WT)
ABAH(WT)
D
Day 7 MPO-/- vs WT Striatum
No.of BrdU(+) Cells/Field
100
80
60
40
20
0
***
ns
ns
ns
Sham (MPO-/-)
Vehicle (MPO-/-)
ABAH (MPO-/-)
Sham (WT)
Vehicle (WT)
ABAH (WT)

Figure 7

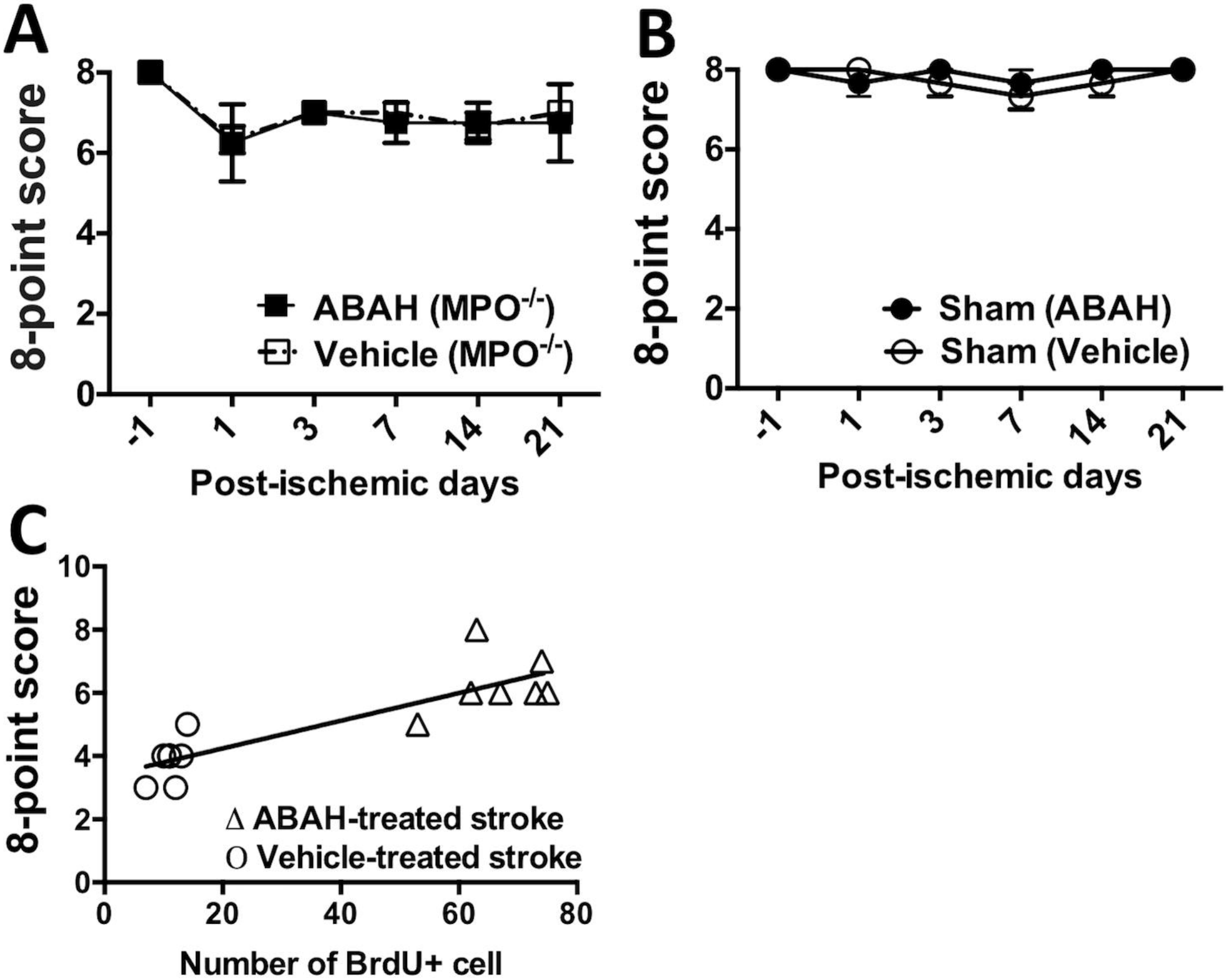
A
8-point score
8
6
4
2
0
ABAH (MPO-/-)
Vehicle (MPO-/-)
-1
1
3
7
14
21
Post-ischemic days
B
8-point score
8
6
4
2
0
Sham (ABAH)
Sham (Vehicle)
-1
1
3
7
14
21
Post-ischemic days
C
8-point score
10
8
6
4
2
0
Δ ABAH-treated stroke
O Vehicle-treated stroke
0
20
40
60
80
Number of BrdU+ cell

Figure 8

[JPET # 235127]

Myeloperoxidase inhibition increases neurogenesis after ischemic stroke

HyeonJu Kim, Ying Wei, Ji Yong Lee, Yue Wu, Yi Zheng, Michael A. Moskowitz, and John W. Chen

Running title: MPO inhibition increases neurogenesis after stroke

Center for System Biology and Institute for Innovation in Imaging, Massachusetts General Hospital, Harvard Medical School, Boston, 02114.

Affiliations:

Center for System Biology and Institute for Innovation in Imaging, Massachusetts General Hospital, Harvard Medical School, Boston, MA: (H.-J.K., J.-Y.L., J.W.C)

Neuroscience Center, Massachusetts General Hospital, Harvard Medical School, Boston, MA: (W.Y., Y.W., Y.Z., M.A.M).

The Journal of Pharmacology and Experimental Therapeutics

Corresponding author:

John W. Chen, MD, PhD
Massachusetts General Hospital, Harvard Medical School
Richard B. Simches Research Center
185 Cambridge Street
Boston, MA, 02114, USA
Tel: 617-643-7071
Fax: 617- 643-6133
E-mail: Jwchen@mgh.harvard.edu

SUPPLEMENTARY FIGURES:

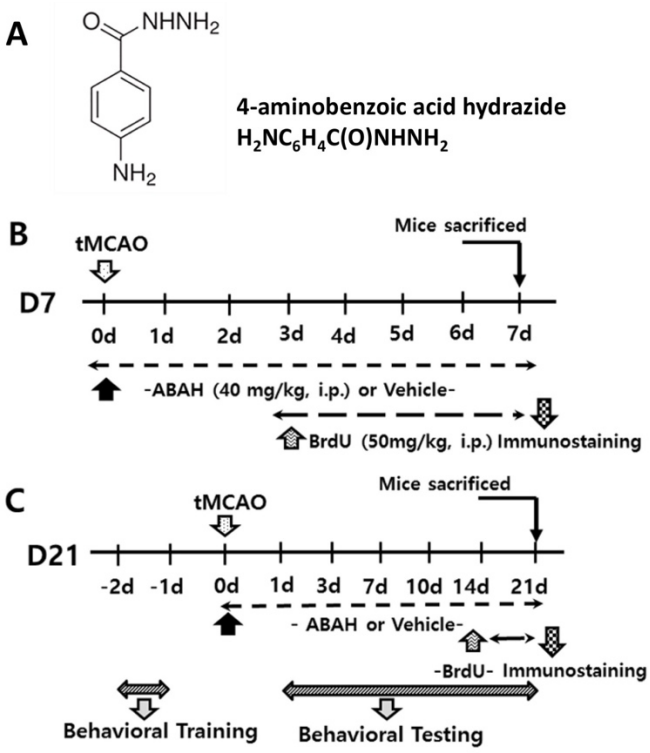

Supplementary Fig. 1. (A) Chemical structure of 4-aminobezoic acid hydrazide.

(B) A schematic diagram of experiments on day 7 after stroke: Mice were treated twice daily with intraperitoneal injections of either 4-aminobenzoic acid hydrazide (ABAH, 40 mg/kg body weight) or vehicle, starting immediately after tMCAO and sacrificed on day 7 after stroke. To label dividing cells, mice were intraperitoneally injected with bromo-2'-deoxyuridine (BrdU) (50 mg/kg, i.p.) twice daily from days 3 to 7 after ischemia. (C). Experimental scheme for day 21 after stroke: Mice were treated with the same conditions in (A) with ABAH treatment administered to day 21 after stroke. Mice were injected with BrdU from days 14 to 21 after ischemia, and sacrificed on day 21. Behavioral test was performed with pre-training and 8-point neurological test up to day 21 after stroke. Immunostaining sample was collected on day 21 after stroke.

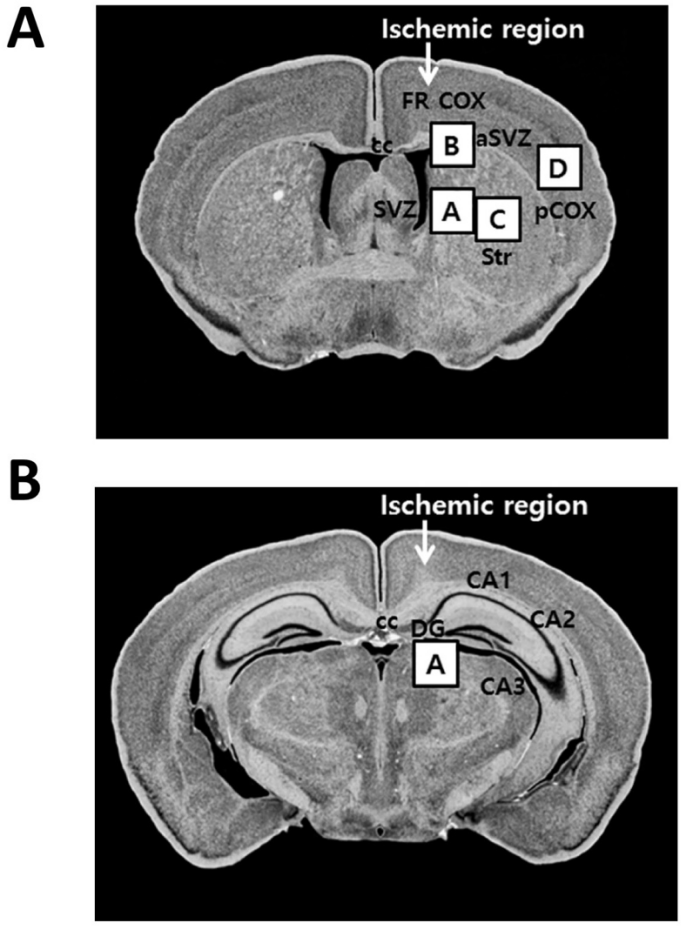

Supplementary Fig. 2. Schematic diagram of the anatomic locations utilized for immunohistochemistry in tMCAO. (A) shows the regions of the SVZ, aSVZ, striatum and parietal cortex used for immunohistochemical examinations (as shown in boxes, A-D) in a brain section after tMCAO. SVZ, subventricular zone; aSVZ, anterior subventricular zone; Str, striatum; FR COX, frontal cortex; CC, corpus callosum; pCOX, parietal cortex. (B) shows the area in the hippocampal dentate gyrus used for immunohistochemical examinations (as shown in box, A). DG, dentate gyrus; CC, corpus callosum.

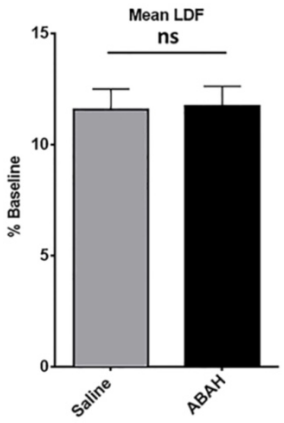

Supplementary Fig. 3. Laser Doppler Flowmetry (LDF) measurements after stroke. Vehicle (n=30) and ABAH (n=30). ns=not significant.

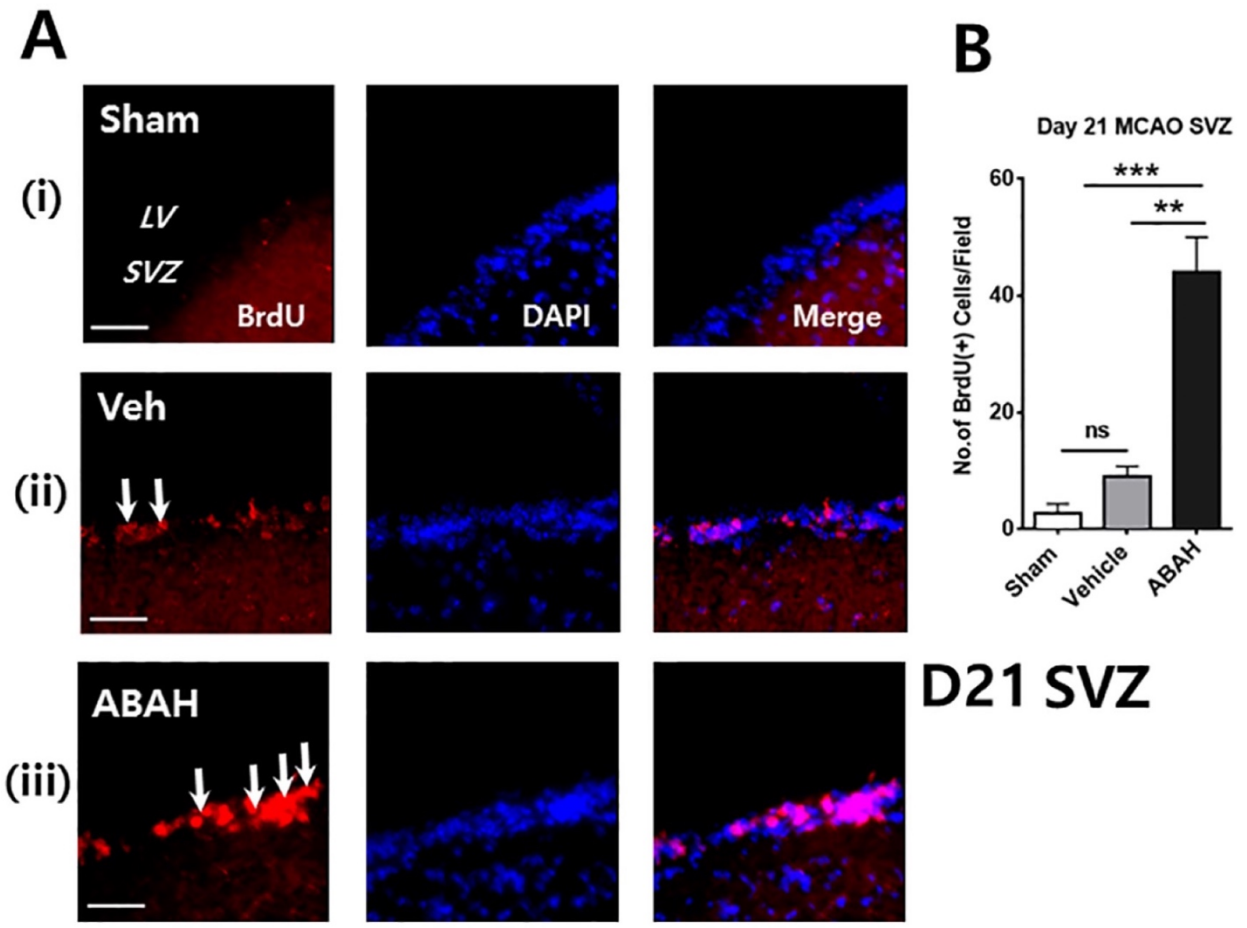

Supplementary Fig. 4. MPO inhibition increased the number of $BrdU^+$ cells in the ischemic SVZ on day 21 after tMCAO. (A) BrdU staining in the ipsilateral SVZ in sham, vehicle-treated, and ABAH-treated tMCAO mice. $BrdU^+$ (red), $DAPI^+$ (blue). Merge ($BrdU^+$/$DAPI^+$). LV: lateral ventricle, SVZ: subventricluar zone. Arrows identify BrdU-positive cells. (B) Quantification of (A). Sham, vehicle- and ABAH-treated mice (n=3 in each group). Magnification, ×40. Scale bar, 50 μm. Data are mean ± SEM. ANOVA followed by Bonferroni's *post-hoc* test. *** $p < 0.001$.